AN INVESTIGATION OF THE S/N FATIGUE LIFE GAGE

by

DAVID H. JOHNSON

B.S. United States Naval Academy
(1958)

SUBMITTED IN PARTIAL FULFILLMENT OF THE
REQUIREMENTS FOR THE DEGREES OF
MASTER OF SCIENCE
AND
NAVAL ENGINEER

at the
MASSACHUSETTS INSTITUTE OF TECHNOLOGY
June 1967

AN INVESTIGATION OF THE S/N FATIGUE LIFE GAGE

by

DAVID H. JOHNSON

B.S. United States Naval Academy
(1958)

SUBMITTED IN PARTIAL FULFILLMENT OF THE
REQUIREMENTS FOR THE DEGREES OF
MASTER OF SCIENCE
IN NAVAL ARCHITECTURE AND MARINE ENGINEERING
AND
NAVAL ENGINEER

at the
MASSACHUSETTS INSTITUTE OF TECHNOLOGY
June 1967

Signature of Author _____
Department of Naval Architecture and
Marine Engineering, May 19, 1967

Certified By _____
Thesis Supervisor

Certified By _____
Reader for the Department

Accepted By _____
Chairman, Departmental Committee
on Graduate Students

AN INVESTIGATION OF THE S/N FATIGUE LIFE GAGE

by

David H. Johnson

Submitted to the Department of Naval Architecture and Marine Engineering on May 19, 1967, in partial fulfillment of the requirements for the Master of Science Degree in Naval Architecture and Marine Engineering and the Professional Degree, Naval Engineer.

ABSTRACT

The S/N fatigue life gage is an electrical sensor similar to a foil strain gage which was designed to measure fatigue damage or fatigue life. The gage accumulates information on fatigue by exhibiting a permanent change in gage resistance which is cumulative, irreversible and reproducible.

This thesis set out to investigate the gage macroscopically and microscopically in order to further understand the mechanism by which it functions and some of its peculiarities. Constant deflection, reverse bending tests were conducted of 1018 CR steel, aluminum and acrylic plastic.

The results gave good correlation with predicted gage performance curves. The mechanism by which the gage operates is not limited to cold working, but also crack propagation. The fatigue gage can be used as a strain gage with reasonable accuracy in the low cycle fatigue range. After subjecting the gage to fatigue there appears to be an increase in resistance at no load as a function of time. The tests on "Lucite 129" seem to yield an endurance limit of about 1900 $\mu\epsilon$ for constant strain fatigue.

This paper discusses some of the gage peculiarities and gives recommendations for further investigation.

Thesis Supervisor: W. M. Murray

Title: Professor of Mechanical Engineering

ACKNOWLEDGMENTS

I wish to express my appreciation to Professor W. M. Murray for introducing me to this investigation and for his assistance and encouragement.

I wish to thank Mr. R. J. Whitehead of W. T. Bean, Inc. and Mr. J. E. Starr of Micro-Measurements, Inc. for their cooperation in providing part of the test equipment and test specimens.

I wish to thank Mr. Ross Melton and Mr. Art Gregor for their advice concerning strain gage instrumentation and metallography, respectively.

I wish to thank Mr. Regis Pelloux of the Boeing Company for his thoughts and references concerning the behavior of metals.

And, above all, I wish to thank my lovely wife, Kaywin, for her patience, devotion and ability to decipher the handwritten manuscript for typing.

TABLE OF CONTENTS

INDEX OF FIGURES

SYMBOLS AND DEFINITIONS

A - cross sectional area

dA - increment of cross sectional area

C_n - constants

c - distance from neutral axis to extreme fiber

E - Young's modulus of elasticity

GF - gage factor; sometimes called strain sensitivity factor

I - moment of inertia

L - length

M - bending moment

N - number of cycles

P - load

R - electrical resistance

Rg - gage resistance

ΔR - increment of resistance; also amount of "zero shift"

t - time

x - arbitrary distance

y - beam deflection

y' - first derivative of y with respect to x

y'' - second derivative of y with respect to x

ϵ - strain

ϵ_c - compressive strain

ϵ_m - mean strain

ϵ_R - cyclic strain

ϵ_t - tensile strain

ϵ_T - total strain range

$\Delta\epsilon$ - increment of strain

μ - micro units or 10^{-6}

$\mu\epsilon$ - microstrain (10^{-6} in./in.)

ϱ - electrical resistivity

ω - angular speed

CPM - cycles per minute

psi - pounds per square inch

I. INTRODUCTION

The recognition of material failures by a mechanism called fatigue* is by no means new to the twentieth century (2); however, the development of sensor devices to predict fatigue failure is rather recent. Fatigue sensor devices date back to about 1948 (15), and today at least two companies market these devices. One such device is THE S/N** FATIGUE LIFE GAGE which was developed by Harting (15) (16). The fatigue gage is manufactured by Micro-Measurements, Inc. and is marketed by M. T. Bean, Inc. This investigation is confined to the particular gage shown in Figure XVII, Section V. A description of the gage can be found in Appendix C.

The fatigue gage was developed to measure cumulative fatigue damage of a material by noting the resistance change of a gage which is bonded to the surface of the material. The resistance change is also a cumulative

---

* A review of fatigue theory is beyond the scope of this investigation; however, Avery (2) has a good bibliography and Manson (20) has good discussion of the subject.

** Trademark: Micro-Measurement, Inc., Romulus, Michigan. Throughout this investigation reference will be made as "the fatigue gage".

effect and changes in an irreversible, predictable manner. For example, if the gage was mounted on a specimen, cycled in reverse bending at constant strain amplitude, and the resistance was plotted as a function of the number of cycles on a log-log plot, the result should be a series of curves as shown in Figure I. These curves can then be correlated to the fatigue life of a specimen.

Harting concluded during the gage development that large resistance changes (on the order of 300%) were due to gage cracking and small resistance changes (on the order of 1 or 2%) (16) were due to work hardening* of the grid material. He further concluded that the gage could be designed to change resistance in a predictable fashion by work hardening, cracking or both. Oldroyd, Burns, and Benham (23) support this idea by stating that materials with a ultimate/yield strength ratio greater than 1.4 cyclic hardening occurs and those for which this ratio is less than 1.2 cyclic softening occurs.

Chironis (7) states that the S/N fatigue gage works on the principal of work hardening of the grid material.

---

* Chalmers and King (5, 6) have a detailed discussion of the subject.

FIGURE I

S/N FATIGUE LIFE GAGE PERFORMANCE CURVES

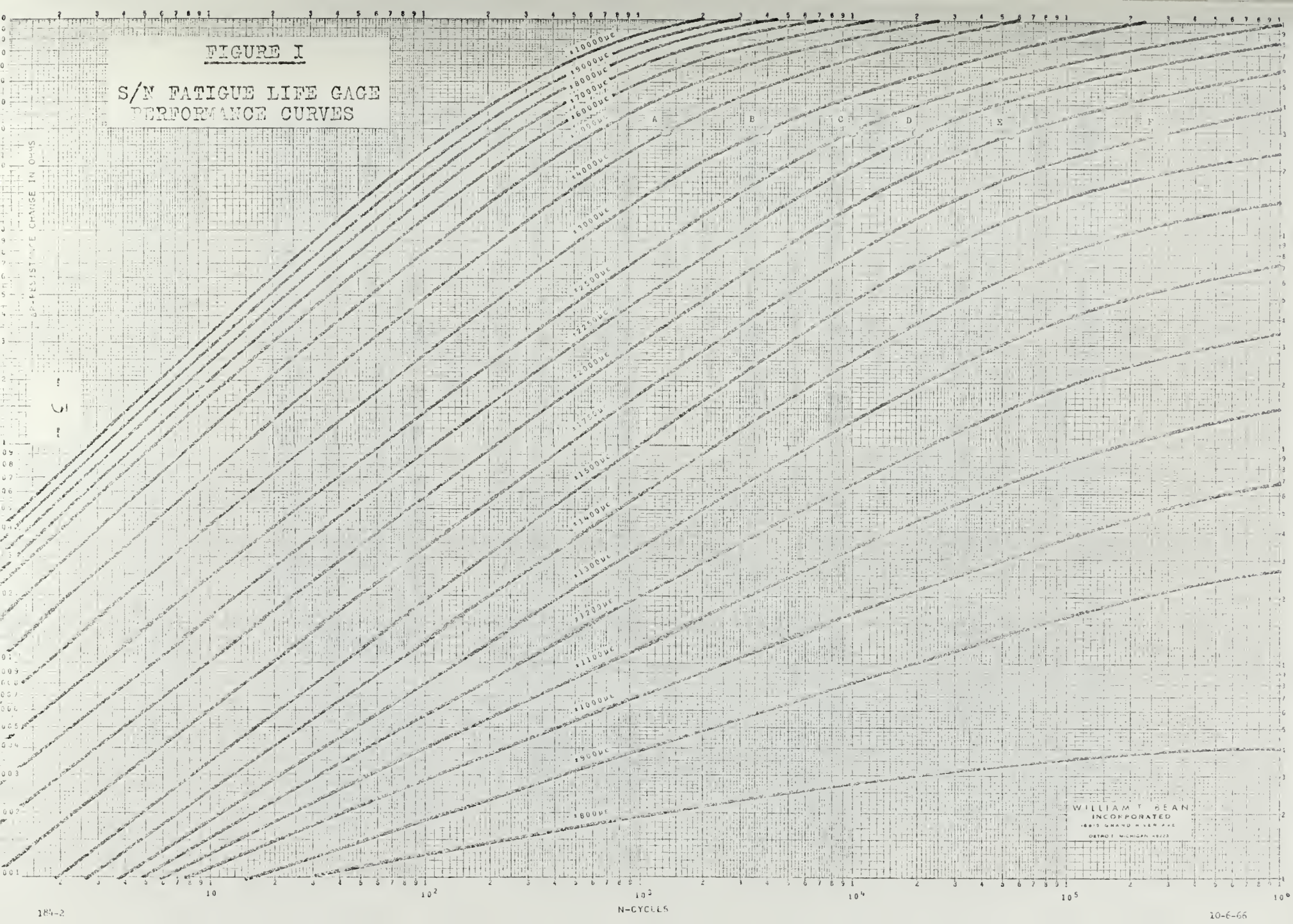

184-2

10-6-66

Webeler (33) concluded that fatigue of disordered alloys produces cold-work regions which are macroscopic, and hence cause an increase in resistivity due to electron scattering. He did not observe microcracks as resistivity increased. Cohen (9) also noted that the resistivity of a disordered alloy showed a shallow maximum as a function of cold working; however, he also cites two examples, a nickel-alloy and a copper alloy, which show continously decreasing resistivity as a function of cold working.

The material used in the foil grid of the fatigue gage is constantan. There has been no information published concerning the change in resistivity of constantan foil as a function of cold working. Boeing (4) conducted tests on annealed constantan, but no definite conclusions were reached concerning the change in resistivity as a function of cold working.

Up to this point it has been assumed that cold working causing a change in resistivity describe the mechanism by which the fatigue gage operates. It is certainly possible that other mechanism may come into play.

The resistance of an electrical conductor has been expressed by Kelvin as:

$$R = \rho \frac{L}{A} \qquad (1)$$

where

R = resistance, in length L (ohms)
ρ = resistivity or specific resistivity (ohm-in.)*
L = length of conductor (in.)
A = area of cross section ($in.^2$)

Equation (1) assumes that the conductor is homogeneous, the cross-sectional area is constant and small compared to the length (L), the current is continous and uniformly distributed. Equation (1) can be expressed somewhat differently by taking the logarithm of both sides and differentiating: hence,

$$\frac{dR}{R} = \frac{d\rho}{\rho} + \frac{dL}{L} - \frac{dA}{A} \qquad (2)$$

which expresses the unit change in resistance in terms of the unit changes in resistivity, length and cross-sectional area. Equation (2) states that an increase in resistance can be achieved by increasing resistivity, increasing length and/or decreasing cross-sectional area. Instead of the differentials of equation (2), one could think in terms of many small finite elements, and that the summation of these elements would compose one strand or even a whole gage.

---

* $\rho = 19.3\ \mu$ ohm-in. for wrought constantan @ $20^{\circ}C$

If a fatigue gage was mounted on a specimen and the specimen was returned to the same strain for each resistance measurement, the dL term of equation (2) would be zero. Under this condition the resistance change can be expressed by

$$\frac{dR}{R} = \frac{d\rho}{\rho} - \frac{dA}{A} \qquad (3)$$

It must be noted that a change in area may also cause a change in resistivity. Dahl (10) showed that for a small reduction in area there was no change in resistivity; however, for a large reduction in area there was an increase in resistivity.

Horne (17) compared a bonded fatigue gage optically before and after strain hardening and found no dimensional change even though the gage resistance increased. The type of dimension change suggested by equation (3) may not be noticed by an observation such as Horne's. To detect the incremental change suggested by equation (3) would probably require investigations using metallography. If the epoxy surface could be removed from the fatigue gage, much valuable information could be quickly obtained with a scanning electron microscope such as manufactured by JEOLCO*.

---

* Trademark: Japan Electron Optics Laboratory Co. Ltd.

There is indication in the literature that during fatigue or even during fracture, a homogenous media does not exist. It has been recognized for sometime that during fatigue, electron emission occurs. Bennett (3) has noted the libration of gas from fatigued aluminum. Furuichi, Fuji and Mizukawa (13) have observed pitting at the grain boundaries in HCP metals during fatigue. Thompson (30) also noticed pitting in some FCC metals, including copper. Considering the above observations, the term dA in equation (3) may play an important part when considering a number of finite elements of area. The variation in area would possibly be caused by creation of internal voids or pits, or even cracks. This would add an additional mechanism to the fatigue gage operation, in addition to any change in resistivity.

Much of the literature does not seem to support the fact that work hardening of FCC metals continue past the first few thousand cycles. Wadsworth (32) found that FCC metals which were soft initially hardened over the first few thousand cycles. If the metal was hard at the start of the test, hardening did not occur. Mott (22) reiterates, in part, the work of Thompson, Wadsworth and Lcuat on fatigue in polycrystalline copper which further supports these observations. Mott points out that the formation of a

crack across a single grain probably takes a good deal less than half the total fatigue life, and the spread of the crack at a gradually increasing rate through the remainder of the specimen takes most of the life. Ebner and Backofen (11) conducted constant deflection, alternating bending tests (strain amplitude of approximately .2%) on copper and found that saturation occurred at about 2000 cycles.

Gibbons (14) accumulated what little data was available in this country concerning strain-cycle fatigue of wrought copper-nickel (70-30). About the only information that proved of any value to this investigation was that an endurance limit* exists at a stress level of approximately 22,650 psi, corresponding to a strain amplitude of about .1%. For strain amplitudes larger than .1% fatigue cracks can be expected.

It must be remembered that during gage manufacturing, it might be most difficult to get "polished" strands in a gage. In the presence of triaxial stresses any notch at the edge of a strand will favor crack development and propagation.

---

* In actuality non-ferrous alloys have no endurance limit. Gibbons' figure is based on 10^7 cycles.

Triebes (31) noticed very good correlation between his tests and Figure I. The fatigue gage does operate in a predictable fashion except for occasional deviation at high number of cycles. Chironis (7) also discusses this deviation, and the phenomena is illustrated in Figure 5 of his article. Although the fatigue gage does give reproducible data, the mechanism by which this occurs should be thoroughly understood. If the mechanism were thoroughly understood, some light might be shed on unexplained phenomena such as the deviation noted by Triebes and Chironis.

II. OBJECTIVES

The primary objectives of this investigation are:

1. To observe and study the S/N fatigue life gage microscopically as well as macroscopically in an attempt to understand the mechanism by which it functions;
2. To relate observed test results conducted on acrylic plastic specimens with the manufacturer's published gage performance data.

The secondary objectives of this investigation are:

1. To observe the use of the S/N fatigue gage as a strain gage;
2. To accumulate constant strain fatigue data for acrylic plastic material;
3. To observe the effect of bending rate or strain rate on the gage performance;
4. To observe the effect of delay in taking data on the gage performance after a test is stopped for:
    a. a short time period,
    b. a long time period.

III. EXPERIMENTAL PROCEDURE

In order to pursue the objectives of this investigation various tests were conducted. These tests were assigned test numbers. When referring to a particular test, reference will be made to the test number or specimen number associated with that test. A description of test equipment can be found in Appendix C.

General Procedure

The bending specimens were selected and prepared as discussed in Appendix A. The clamping block on the S/N fatigue machine which holds the cantilever beam was placed in the appropriate position to attain the desired strain level for the test. The flywheel, which drives an eccentric cam, was positioned so that the cam was in the zero or neutral position for reverse bending of $y = \pm 0.1$ inch. This would correspond to a no load position of a free cantilever beam. The bending specimens were placed in the clamping block for reverse bending. Initial resistance readings were taken with the S/N resistance meter and in some cases, the initial zero reference strain was recorded so that ΔR could be computed as shown in Appendix D. The first 5 cycles were obtained by manually turning the fatigue machine fly wheel. The maximum values of compressive strain and tensile strain were recorded during the first and fifth

cycles by using the S/N fatigue gage as a strain gage in one leg of a half Wheatstone bridge and a decade resistor box in the other leg. (In the case of the aluminum specimens, strain levels were measured using strain gages.) The value of alternating strain used for the test was generally the mean value of the first and fifth cycles, even though other values may have been recorded during the test.

After obtaining the readings for the first and fifth cycles, the variable speed motor driving the fatigue machine was set to run at a predetermined speed. The motor was run until the digital counter indicated the desired number of cycles for the next set of data recording. The fatigue tests were terminated when:

a) the "Lucite 129" failed due to brittle fracture,

b) the steel specimen developed cracks which propagated to the fatigue gage, or

c) the appropriate data had been obtained for the aluminum specimens.

The ΔR data was plotted as a function of N on log-log graph paper in order to compare with the manufacturer's predicted performance and also to indicate areas for further investigation, if correlation were poor.

The strain gages and the fatigue gages were studied during and after the tests. The strain gages could be easily studied microscopically during the tests, but the fatigue gages required much more laborious and elaborate techniques and could only be studied microscopically after the test.

An attempt was made to observe the microstructure of two gages through an optical microscope. Since the fatigue gages were encapsulated in a rather complex epoxy laminate system, there was some doubt if the thin encapsulant might hinder the observation and indeed it did. Both a new gage and a used gage exhibited the same phenomena when viewed through the microscope. The epoxy coating contained numerous randomly oriented glass microfibers. The microscope could not focus on the surface of the metallic grid because of the glass fibers.

To pursue the observation of the grid many hours were spent investigating means and actually trying to remove the epoxy coating covering the grid. The methods which were tried and the results are tabulated below.

TABLE I

RESULTS OF EPOXY REMOVAL METHODS

Method	Results
1. soaked in M. T. Bean epoxy gage stripper for 1 hour at 73°F.	a) no effect on epoxy system

TABLE I (continued)

Method	Results
2. soaked in acetone for approximately 10 hours	a) possibly loosened turret b) one turret fell out c) no effect on epoxy system
3. soaked in hydrofluoric acid for 30 minutes	a) gage curled due to acid attacking glass fibers in backing material b) embrittled backing material c) turned epoxy laminate opaque but no other apparent effect on epoxy system
4. polished with solution of 2 tablespoons of 0.3 micron alumina powder in one pint of distilled H_2O	a) no apparent effect on epoxy system b) not a very good means because of possible damage to the gage
5. soaked in Diversey Diverstrip D-90 epoxy stripper at 70°F for 72 hours.	a) no gross attack of epoxy system b) this was recommended as a very potent epoxy stripper
6. soaked in ECCO Strip 93 for 1 hour at 73°F	a) several micro pits in the epoxy coating when viewed through an optical microscope b) no gross attack of epoxy c) recommended as a very potent and corrosive stripper
7. soaked in Armstrong Epoxy Stripper at 73°F for 120 hours	a) several micropits in epoxy coating when viewed through optical microscope b) no gross attack of epoxy system
8. soaked in Diversey Diverstrip D-90 at 210°F for approximately 10 minutes	a) the stripper evaporated at a very rapid rate and could impose danger to the user due to toxicity, corrosive vapors, etc.

TABLE I (continued)

Method	Results
	b) epoxy system lost its luster, but when viewed through a microscope the coating was still present
9. soaked in Armstrong Epoxy Stripper at 210°F for approximately 20 minutes	a) same precautions as with D-90 b) no apparent effect on epoxy system when viewed through microscope
10. exposed to Hydrochloric acid, sulfuric acid, acetic acid and several common metallurgical etchants	a) no effect on epoxy system

The surface layer of the encapsulant could not be removed by any of the above methods.

Since the surface layer of the encapsulant could not be removed, the next step was to examine the gage by viewing a cross section. A new fatigue gage was cut across the diagonal at approximately 20 degrees with respect to the longitudinal axis (Figure II), then mounted in E-Z Plastic Mount* for polishing, viewing and photographing with a metallograph. This view was chosen because it would show any phenomena in the gage due to transverse as well as longitudinal effects.

---

* Trade name of Dansel Equip. Co., Westboro, Mass.

FIGURE II

DIAGONAL CROSS SECTION OF FATIGUE GAGE

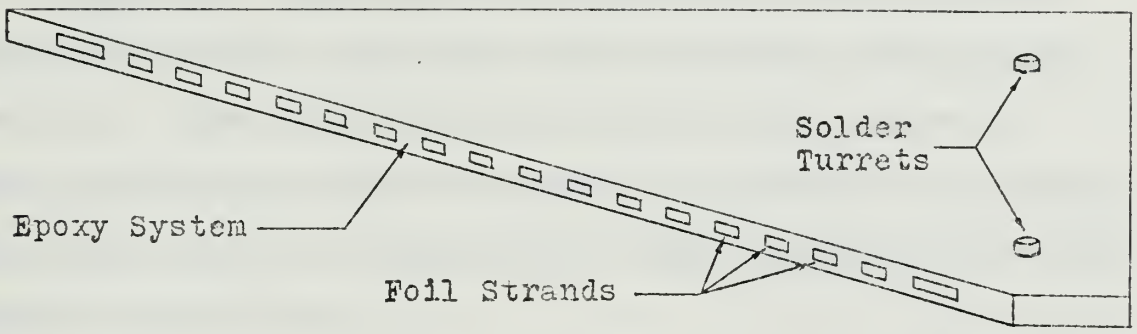

The fatigue gages which were mounted on the Lucite specimens were removed with Armstrong epoxy stripper. In actuality the stripper dissolved the Lucite, but left the gage intact. The gages were cleaned in isopropyl alcohol and mounted in "E-Z" plastic mount. These gages were mounted intact with the transverse direction of the gage vertical and perpendicular to the polishing surface. By mounting the gages in this manner the entire longitudinal portion of one strand could be viewed after polishing; furthermore, it facilitated identifying that point on the gage which was in the field of vision. It was intended to photograph all significant points of interest, but as will be pointed out later, this proved to be most difficult.

Specific Test Procedures

Test # 1: This test was conducted to calibrate the standard specimens for strain level at each clamping block position. Once calibrated, any specimen with the exact same geometry and dimensions could be inserted in the clamping block, and the clamping block could be positioned to the desired strain level.

An aluminum 2024-T4 specimen on which was mounted a strain gage was placed in the clamping block and secured with the gage transverse axis 0.50 inch from the clamp. The gage was connected to the Strainsert strain indicator with an identical gage (dummy gage) in the adjacent leg of a half-bridge. The eccentric cam was rotated to give full beam deflection ($y = \pm 0.10$ inch) in tension and compression. The maximum values of tensile and compressive strains were recorded with the clamping block in positions 1, 2, and 3. The results of the calibration were plotted in Figure III.

Test # 2: This test was conducted to study the zero shift of an EA strain gage of similar size and grid material as the S/N fatigue gage. The only data for fatigue life of this strain gage was given to be 10^5 cycles at $\pm 1500 \mu\epsilon$.

An aluminum 2024-T4 specimen on which was mounted the strain gage was secured in the clamping block with the

block in position # 2 with $\epsilon_R = \pm 3157 \mu\epsilon$. The cantilever was cycled and the gage resistance was measured periodically with the S/N nullmeter. The number of cycles (N) and the gage resistance (Rg) were recorded. After the test was terminated the specimen was studied and photographed with a metallograph. If a crack was observed in the grid strands, the crack length was measured with the metallograph at 1000X thus giving the capability of reading to 2.5×10^{-5} inch. In reference to gage data, "base" refers to the terminal end of gage and "tip" refers to the opposite end.

Test # 3: This test was performed to expand the scope of test # 2. The purpose was to compare strain levels obtained with the S/N fatigue gage with those obtained with a strain gage of similar size and similar grid construction; furthermore, additional information was desired concerning zero shift of the strain gage.

One strain gage and one fatigue gage was mounted on the flat side of an aluminum 2024-T4 specimen and one strain gage was mounted on the bottom directly below the other strain gage. The specimen was secured in the clamping block with the block in position # 2. The specimen was cycled, and the values of gage resistance and indicated strain were measured and recorded at frequent intervals.

As soon as the strain gages showed the first, slightest sign of zero shift, the specimen was removed for initial metallographic observation and study. The specimen was returned to the fatigue machine and placed back into the same position in the clamping block for additional reverse bending cycles. After additional cycles the specimen was again removed for observation. The process was continued until sufficient data of gage resistance, indicated strain levels, and metallographic observations had been obtained.

After seeing the results of Test # 2, cracks in the gage strands were anticipated. The crack lengths were measured during each observation.

Test # 4: This test was conducted to correlate S/N fatigue data of a 1018 CR steel specimen with the manufacturer's performance curves. The specimen contained one fatigue gage which was mounted by W. T. Bean, Inc. This was the only gage which was mounted by the manufacturer. The specimen was secured in the clamping block with the block in position # 1. The specimen was cycled, and the data of indicated strain, number of cycles and gage resistance were recorded. The data of ΔR and N were plotted to compare with the manufacturer's performance predictions which were seen in Figure I.

Test # 5: This test was conducted to correlate S/N fatigue data obtained from a 1018 CR steel specimen with manufacturer's performance curves and to observe the trend in indicated strain when recorded with a fatigue gage over the life of the specimen.

A fatigue gage was mounted on a 1018 CR steel specimen. The specimen was secured in the clamping block with the block in position # 1. A strain indicator was used to determine Rg and ΔR for all cycles less than 300. (Sample computation can be found in Appendix D.) Above 300 cycles the S/N resistance meter was used in place of the strain indicator; however, the strain indicator was used to measure indicated strain. As pointed out previously all indicated strain measurements using the S/N fatigue gage were performed by using the fatigue gage in one leg of a half-bridge and a decade resistor box as the dummy gage in the other leg. The dummy gage resistance was that value of Rg determined from the S/N resistance meter. In this particular test numerous readings of indicated strain were recorded throughout the test.

The speed of the machine was held constant and thus the bending rate was constant at 400 CPM.

Tests # 6 - # 10: These five tests were conducted in similar fashions. One S/N fatigue gage was mounted on each "Lucite 129" acrylic plastic specimen. The specimens were secured in the clamping block, but not necessarily with the transverse axis of the gage at 0.50 inches from the block as in the initial calibration. The clamping block positions are given in Appendix E.

The specimens were cycled in bending at the rate recorded in Appendix E. Values of Rg, ΔR, and indicated strain were recorded at specific intervals of N. In all cases ΔR was plotted as a function of N. In addition, the strain level for each test was plotted as a function of N at failure to obtain a graphical representation of fatigue life of acrylic plastic.

Each gage was removed from the Lucite specimen with epoxy stripper and mounted in plastic as previously explained. All five gages were placed in the same mount. Since one new gage had already been mounted, polished and studied in detail, it was found that this process was extremely time consuming; hence, five gages were placed in one mount. The grid of one gage contains 16 strands; therefore, it was not possible to examine 80 strands within the scope of this investigation. Only several strands and several turrets were examined.

Test # 11: Several specimens were obtained from Triebes (29). Only the history of one specimen could be readily identified. This specimen was a flat bar of 2024-T4 aluminum with one S/N fatigue gage (type NA-01, Lot: A12AP13 or A12AP15) mounted on each side. The values of Rg, ΔR and N, which were recorded in April 1966, were printed on the specimen. In April 1967 the value of Rg was again measured with the S/N resistance meter. This gage an elapsed time of 12 months between readings.

IV. GRAPHICAL RESULTS

FIGURE	
III	S/N FATIGUE MACHINE BLOCK POSITION STRAIN CALIBRATION
IV	COMPARISON OF INDICATED STRAIN FOR FATIGUE GAGE AND STRAIN GAGE
V	PERFORMANCE CURVES FOR SPECIMENS S-1 AND S-2
VI	INDICATED STRAIN OBTAINED FROM S/N FATIGUE GAGE
VII	PERFORMANCE CURVE FOR SPECIMEN L-1
VIII	PERFORMANCE CURVE FOR SPECIMEN L-2
IX	PERFORMANCE CURVE FOR SPECIMEN L-3
X	PERFORMANCE CURVE FOR SPECIMEN L-4
XI	PERFORMANCE CURVE FOR SPECIMEN L-5
XII	"LUCITE 129" FATIGUE CURVE FOR CONSTANT STRAIN

FIGURE III

S/N FATIGUE MACHINE BLOCK POSITION

STRAIN CALIBRATION

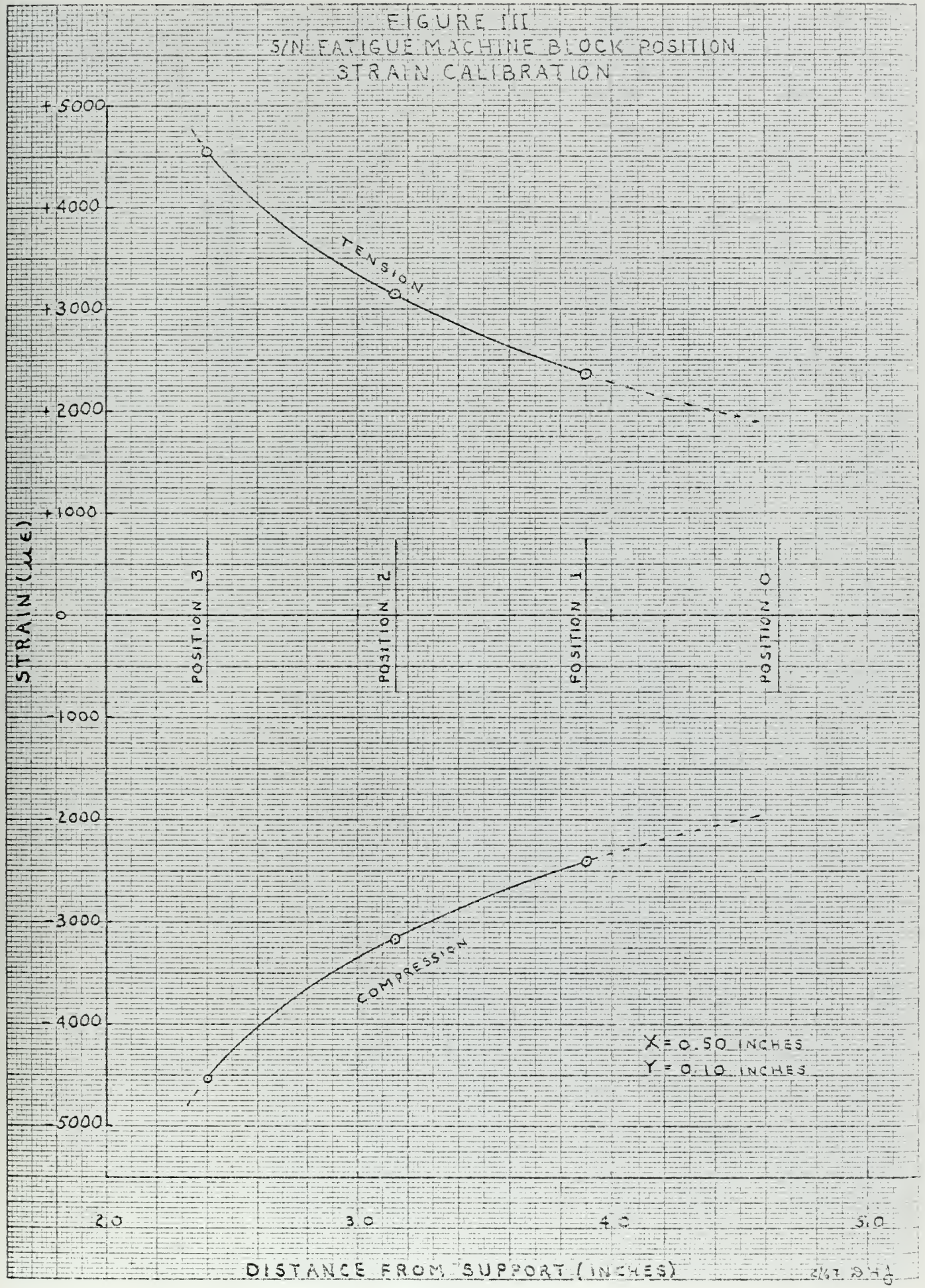

FIGURE IV

COMPARISON OF INDICATED STRAIN FOR FATIGUE GAGE AND EA STRAIN GAGE

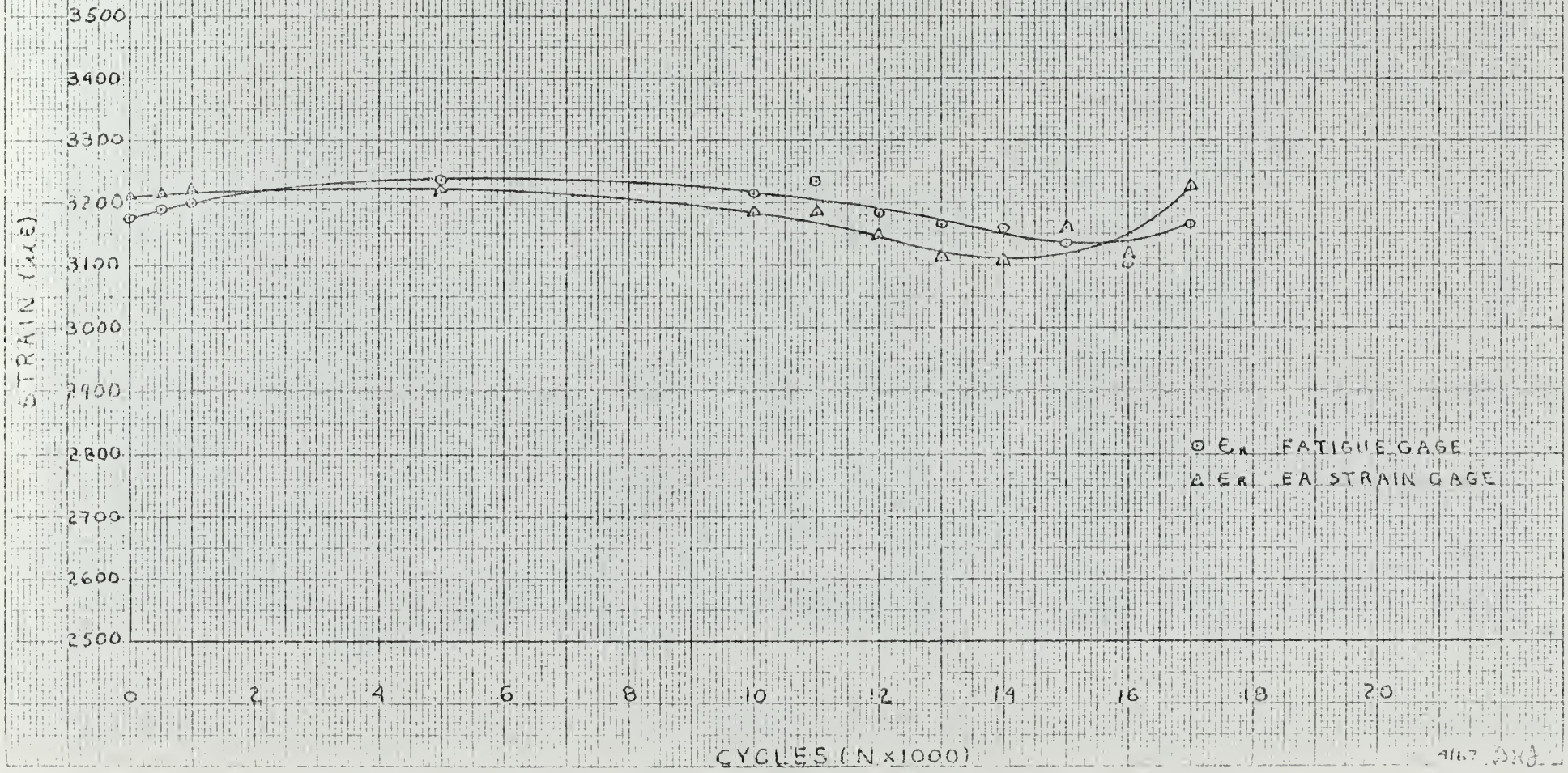

FIGURE V

PERFORMANCE CURVES FOR SPECIMENS

S-1 AND S-2

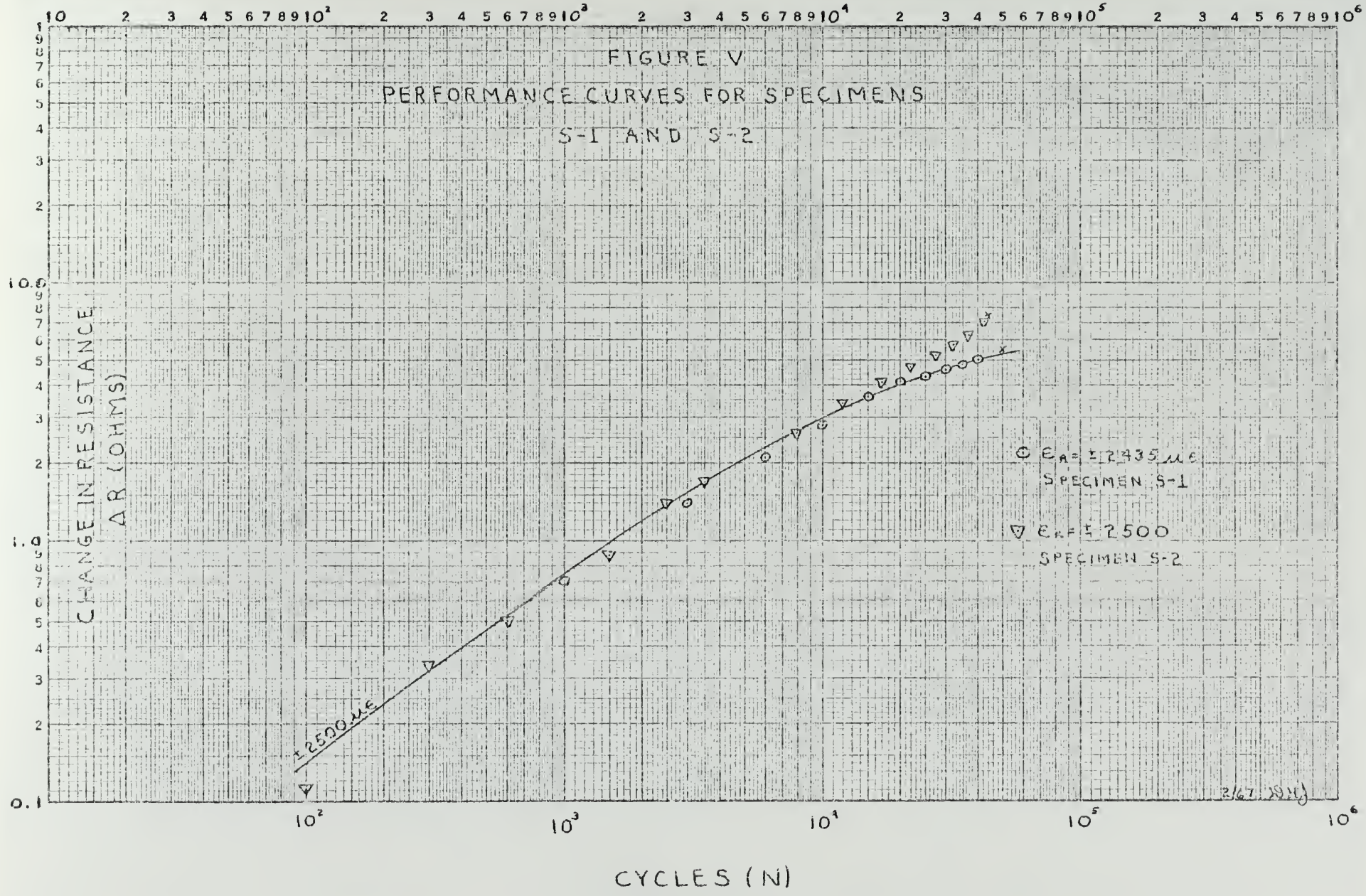

FIGURE VI
INDICATED STRAIN OBTAINED FROM S/N FATIGUE GAGE

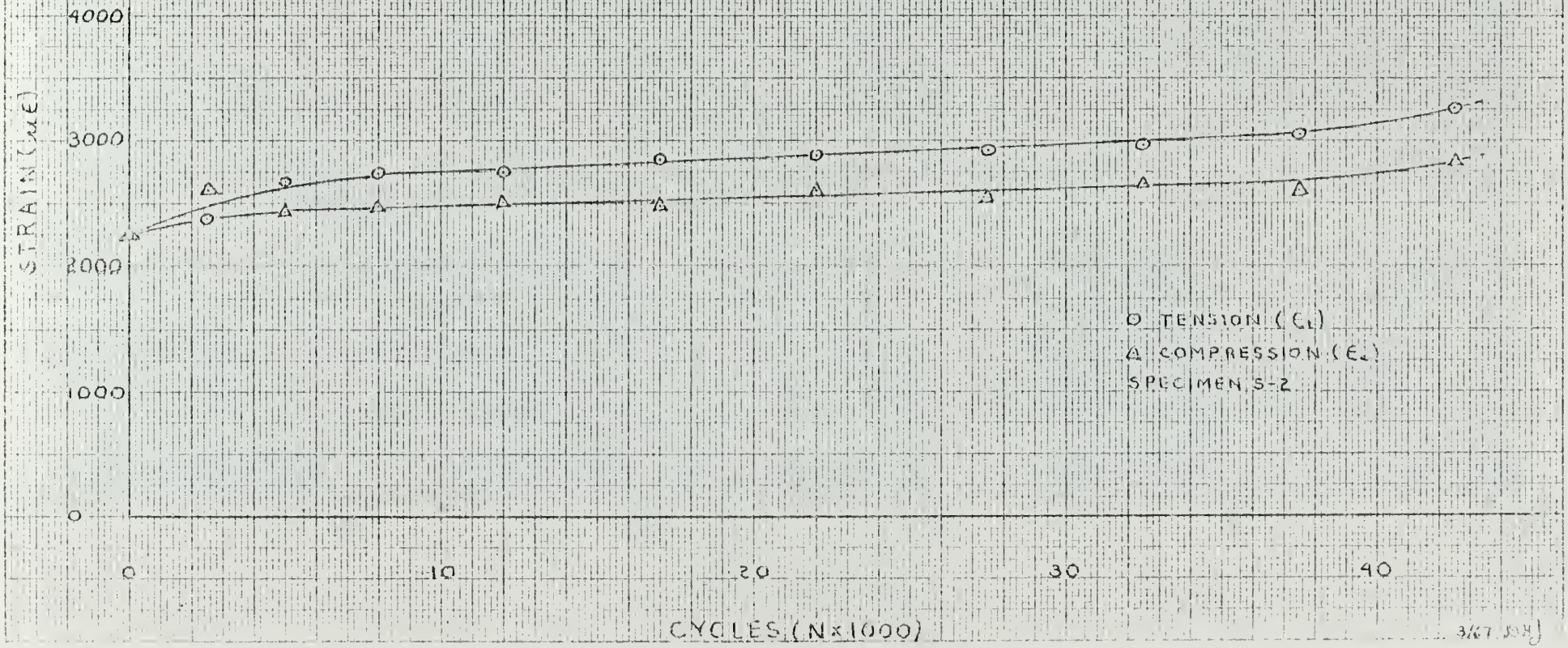

FIGURE VII

PERFORMANCE CURVE FOR SPECIMEN L-1

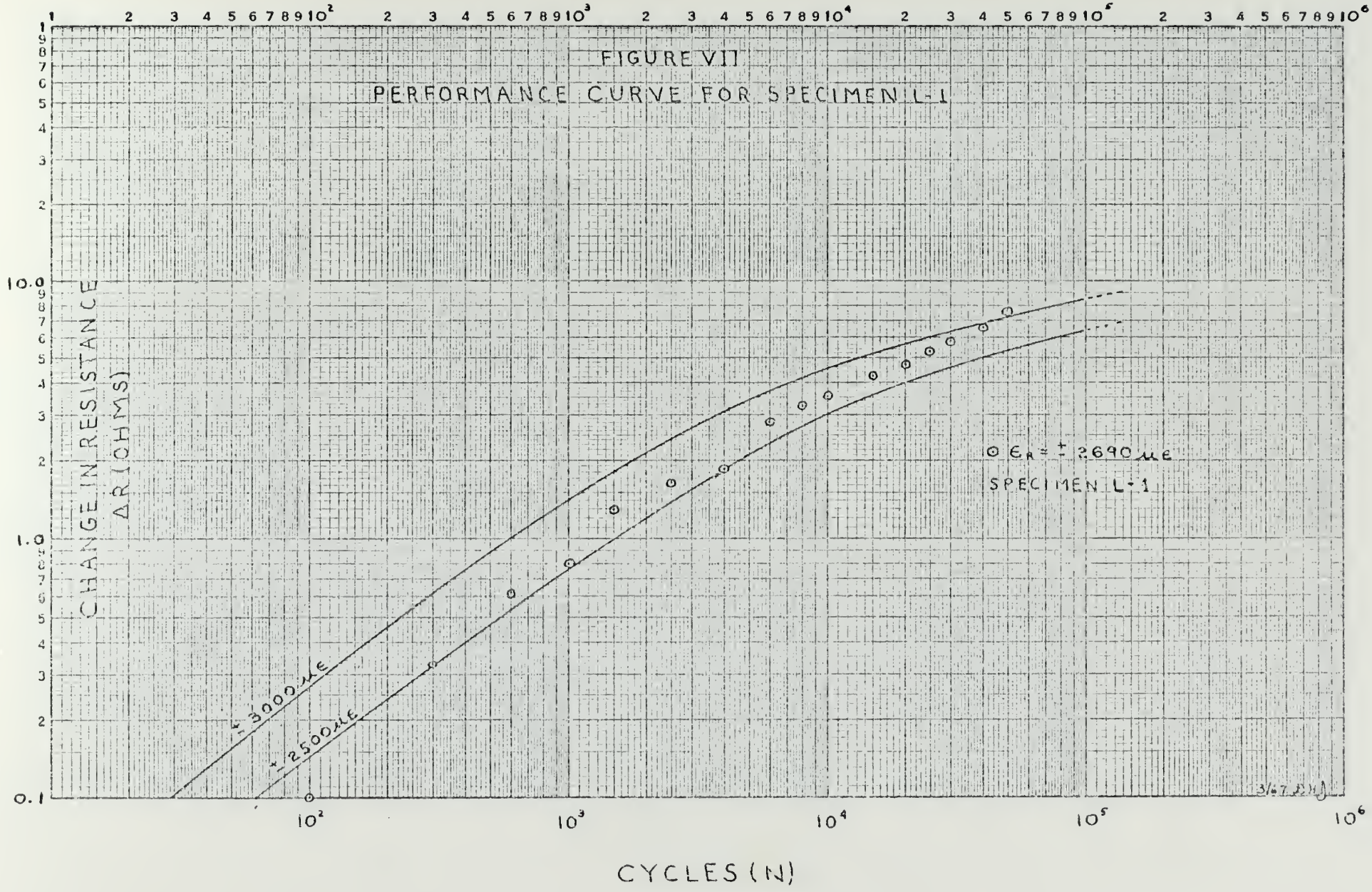

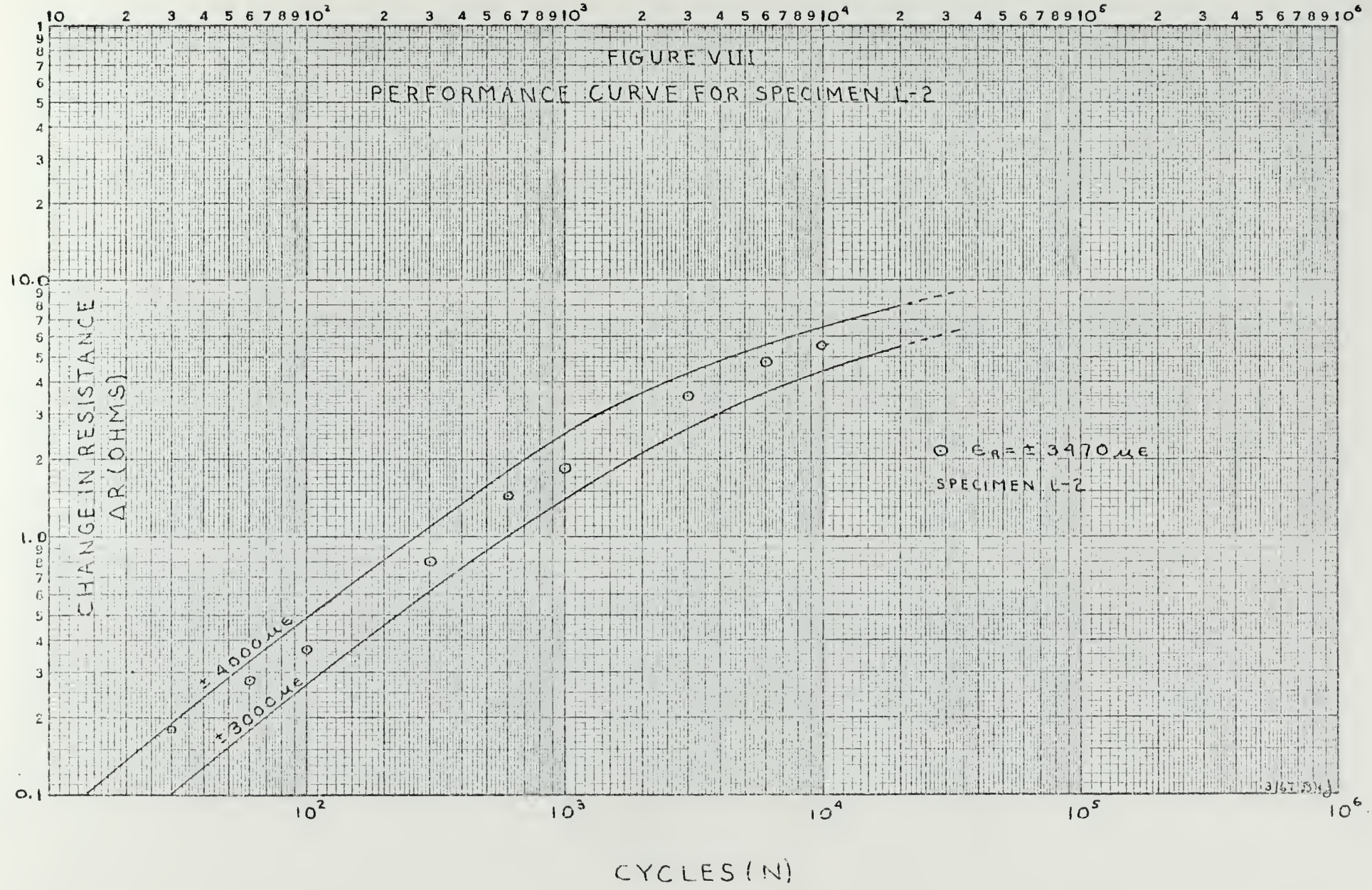
FIGURE VIII
PERFORMANCE CURVE FOR SPECIMEN L-2
CHANGE IN RESISTANCE ΔR (OHMS)
CYCLES (N)
⊙ εR = ± 3470 με
SPECIMEN L-2
± 4000 με
± 3000 με
10
10.0
1.0
0.1
10²
10³
10⁴
10⁵
10⁶

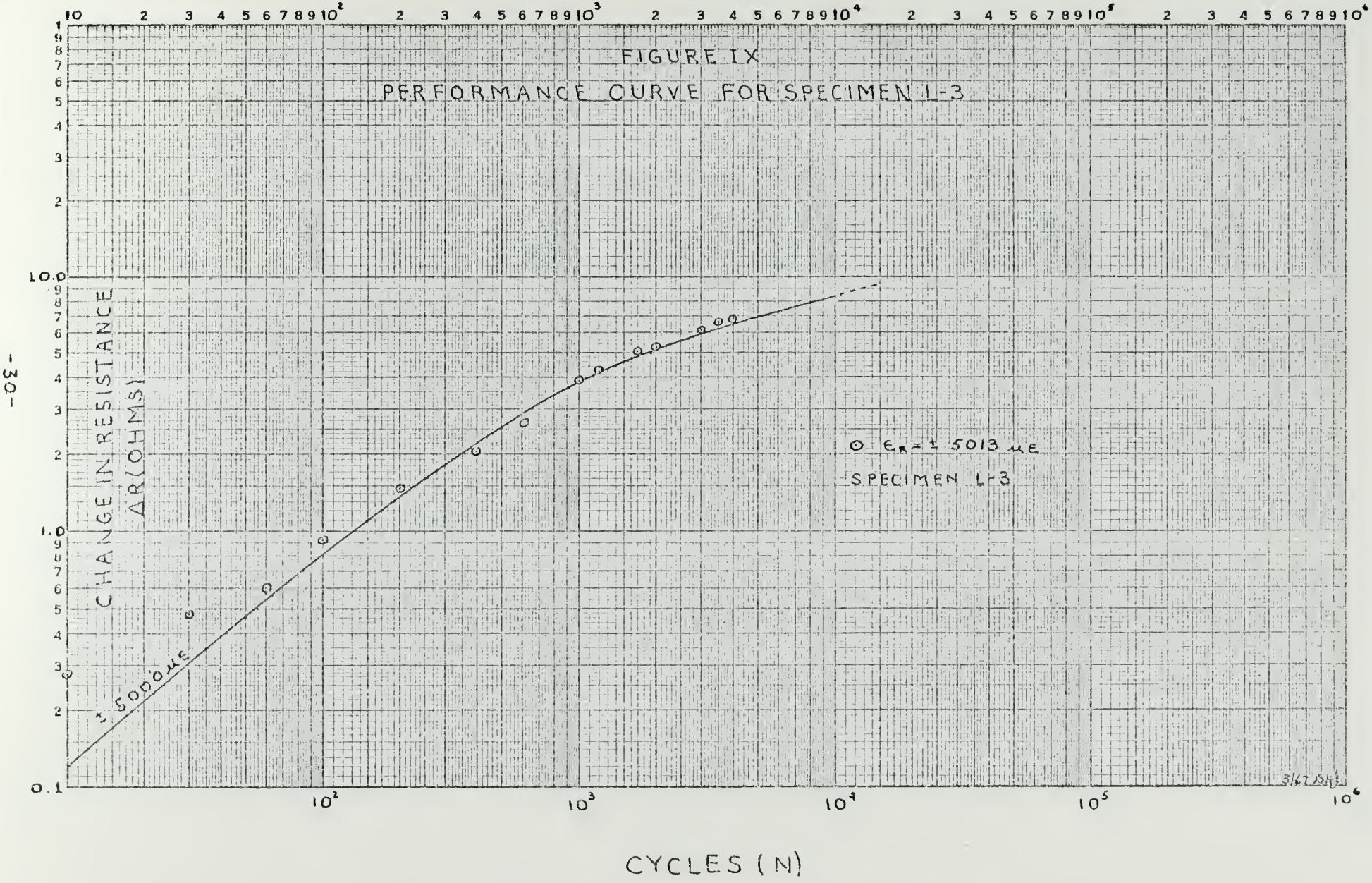
FIGURE IX
PERFORMANCE CURVE FOR SPECIMEN L-3
CHANGE IN RESISTANCE ΔR (OHMS)
CYCLES (N)
⊙ $\epsilon_R = \pm$ 5013 με
SPECIMEN L-3
* 5000με

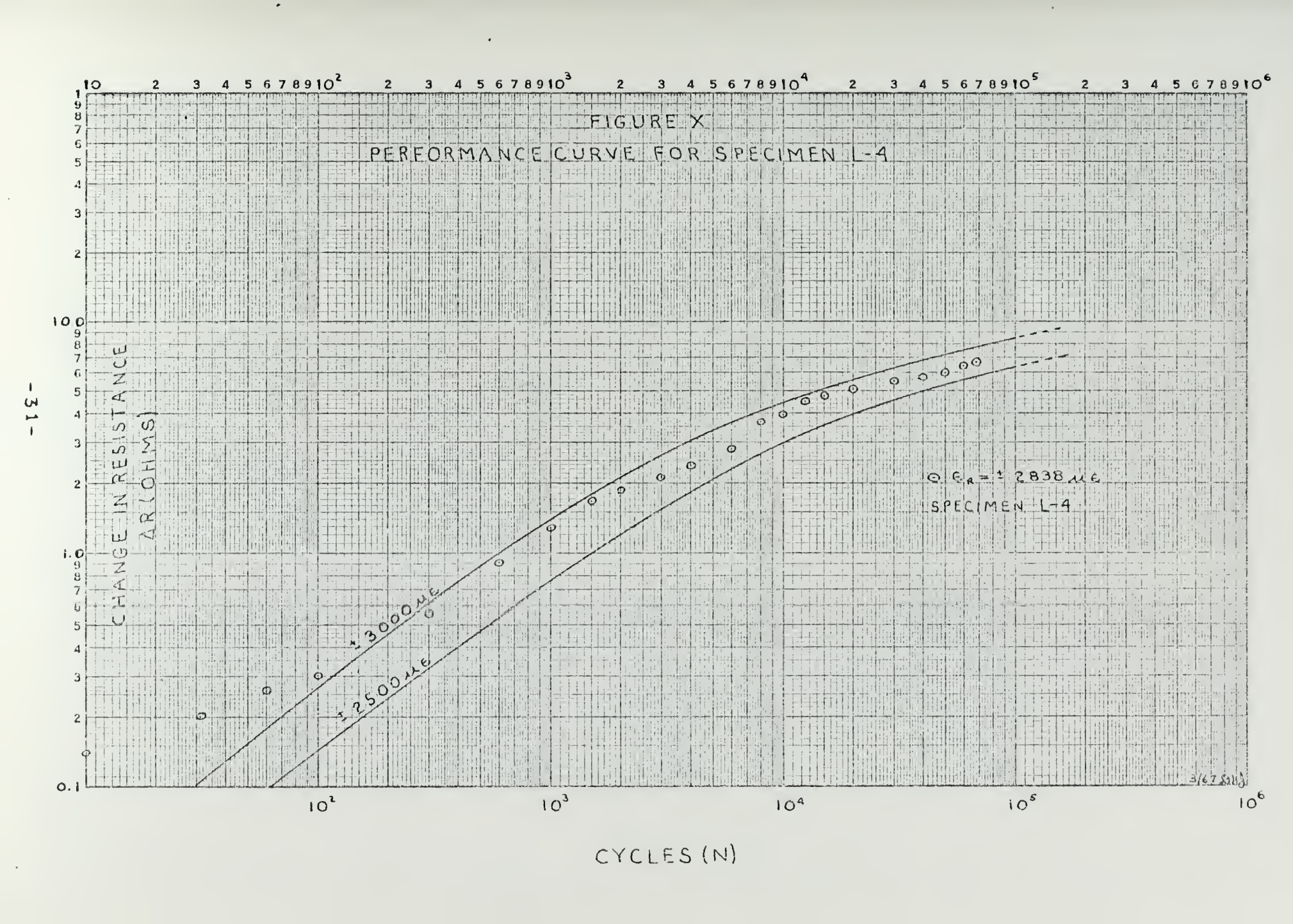
FIGURE X
PERFORMANCE CURVE FOR SPECIMEN L-4
CHANGE IN RESISTANCE ΔR (OHMS)
CYCLES (N)
± 3000 με
± 2500 με
⊙ εR = ± 2838 με
SPECIMEN L-4

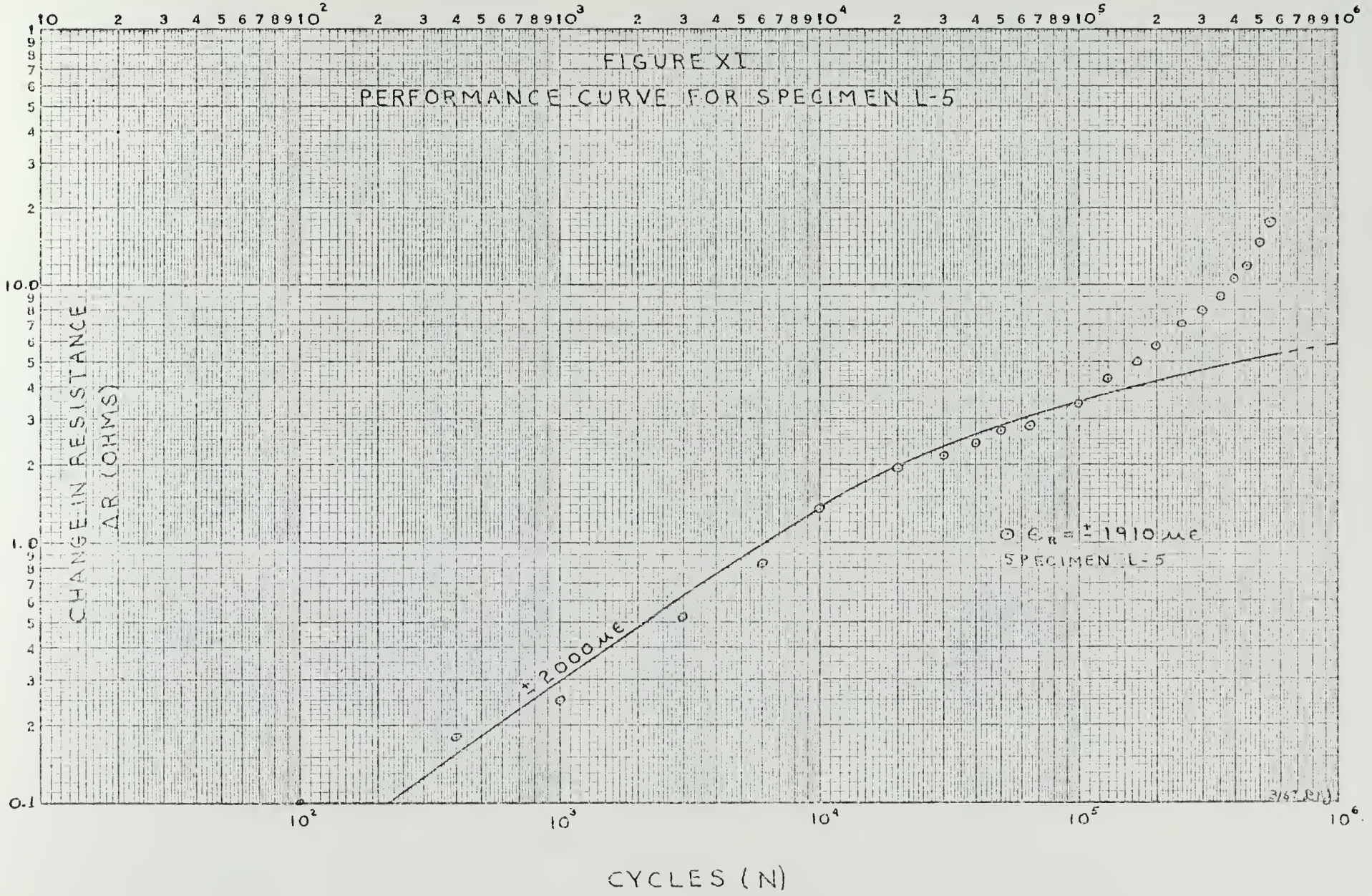
FIGURE XI
PERFORMANCE CURVE FOR SPECIMEN L-5
CHANGE IN RESISTANCE ΔR (OHMS)
CYCLES (N)
± 2000 με
⊙ εR = ± 1910 με
SPECIMEN L-5

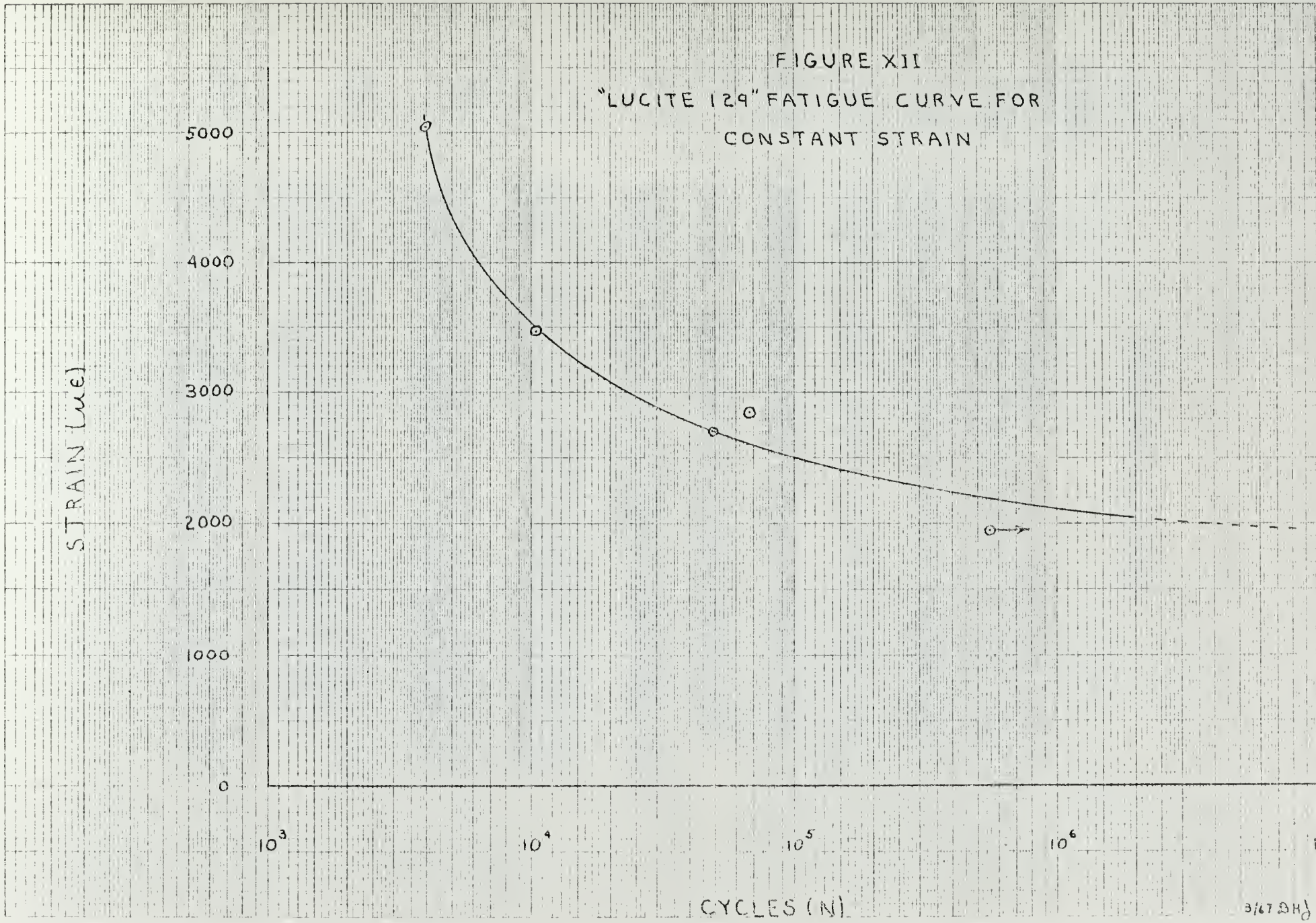
FIGURE XII
"LUCITE 129" FATIGUE CURVE FOR
CONSTANT STRAIN
STRAIN (με)
5000
4000
3000
2000
1000
0
10^3
10^4
10^5
10^6
CYCLES (N)

V. METALLOGRAPH RESULTS

FIGURE	
XIII	CRACKING IN STRANDS OF EA STRAIN GAGE (100X)
XIV	CRACKING IN STRANDS OF EA STRAIN GAGE SHOWN IN FIGURE XIII (200X)
XV	DIAGONAL CROSS SECTION OF S/N FATIGUE GAGE - ZERO CYCLES (100X)
XVI	DIAGONAL CROSS SECTION OF S/N FATIGUE GAGE - LEFT SIDE OF CENTER STRAND IN FIGURE XV (465X)
XVII	DIAGONAL CROSS SECTION OF S/N FATIGUE GAGE TURRET - ZERO CYCLES (100X)
XVIII	DIAGONAL CROSS SECTION OF S/N FATIGUE GAGE TURRET - SAME VIEW AS FIGURE XVII (100X)
XIX	LONGITUDINAL CROSS SECTION OF S/N FATIGUE GAGE TURRET - SPECIMEN L-2, AFTER 10,690 CYCLES AND TERMINAL WIRE REMOVED (100X)
XX	LONGITUDINAL CROSS SECTION OF S/N FATIGUE GAGE STRAND AFTER POLISHING TO DEPTH OF 9.84×10^{-4} INCH - CRACK ROOT OF SPECIMEN L-3 AFTER 4020 CYCLES (1000X)
XXI	LONGITUDINAL CROSS SECTION OF S/N FATIGUE GAGE AFTER SLIGHT POLISHING OF STRAND AT OUTER EXTREMITY - SPECIMEN L-1 AFTER 49,528 CYCLES (1000X)
XXII	LONGITUDINAL CROSS SECTION OF S/N FATIGUE GAGE AFTER SLIGHT POLISHING OF STRAND AT OUTER EXTREMITY AND NEAR INSIDE RADIUS AT END OF STRAND - SPECIMEN L-2 AFTER 10,690 CYCLES (1000X)
XXIII	LONGITUDINAL CROSS SECTION OF S/N FATIGUE GAGE AT INSIDE RADIUS OF STRAND - TIP END OF GAGE - SPECIMEN L-5 AFTER 550,000 CYCLES (500X)

FIGURE XIII

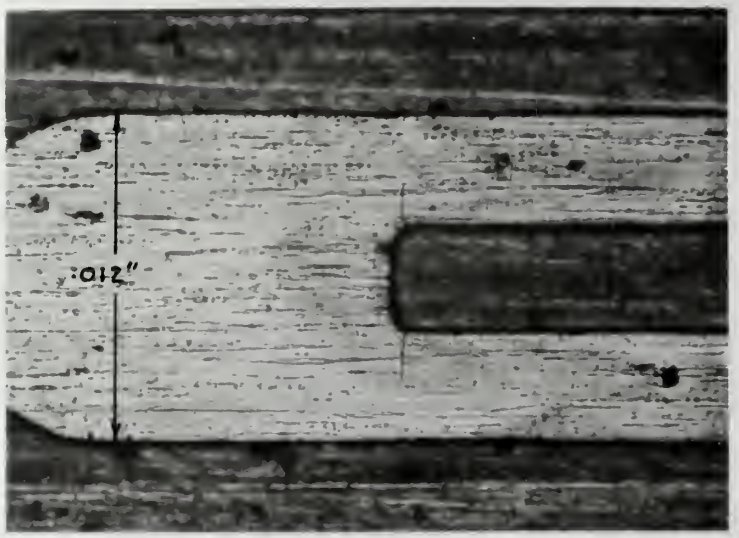

FIGURE XIV

FIGURE XV

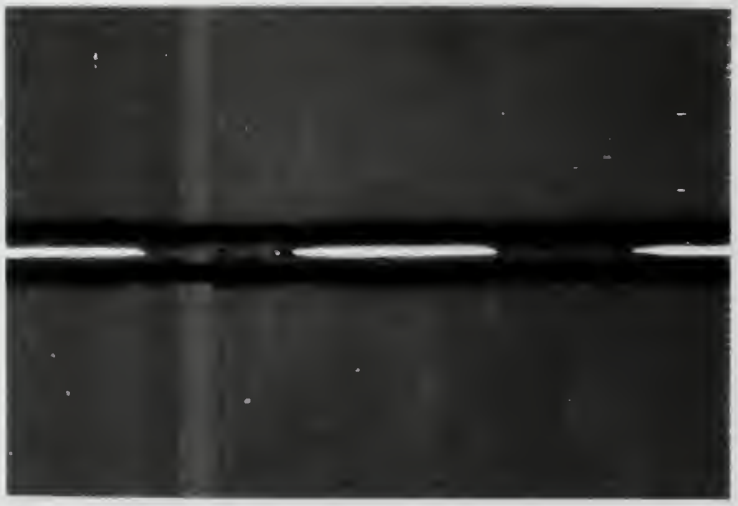

FIGURE XVI

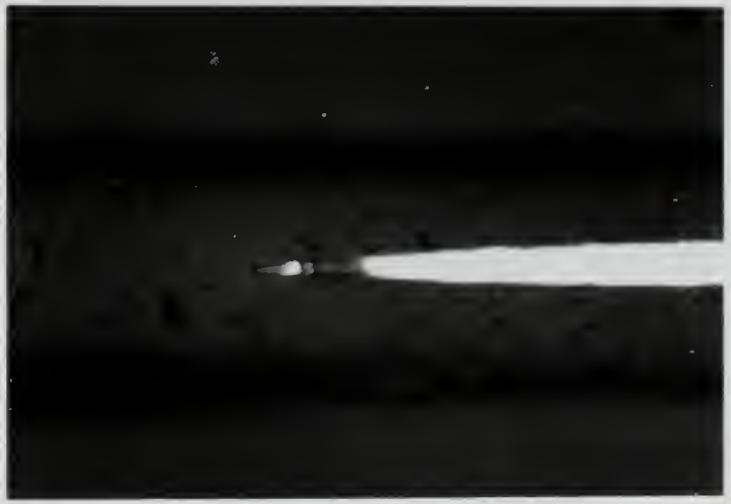

FIGURE XVII

FIGURE XVIII

FIGURE XIX

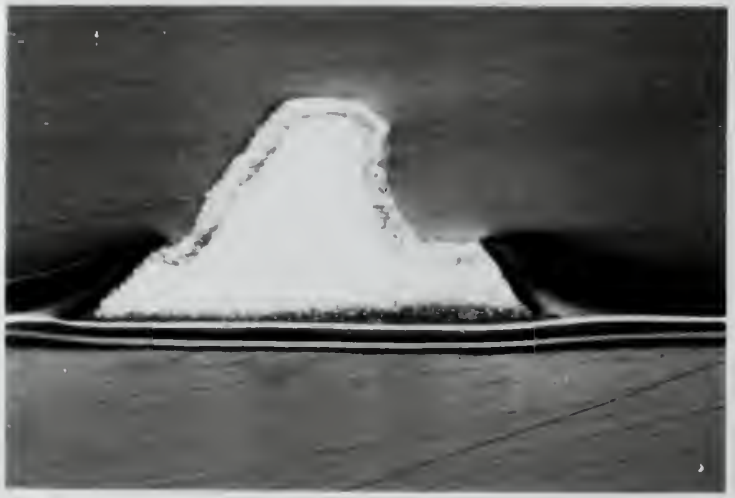

FIGURE XX

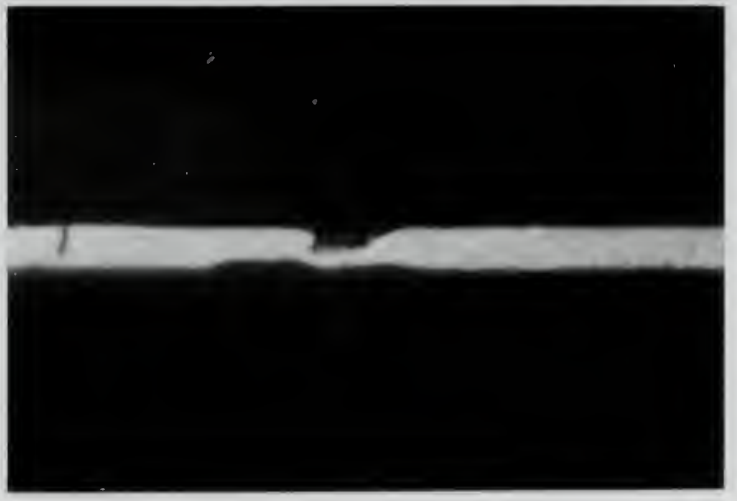

FIGURE XXI

FIGURE XXII

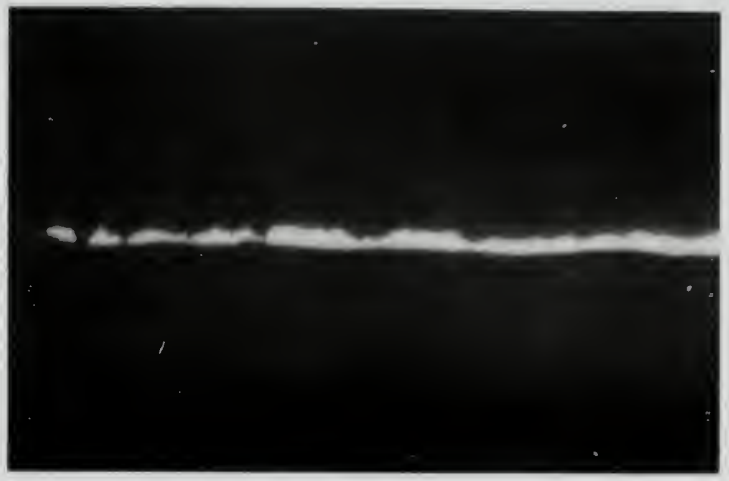

FIGURE XXIII

FIGURE XXIV

FIGURE XXV

FIGURE XXVI

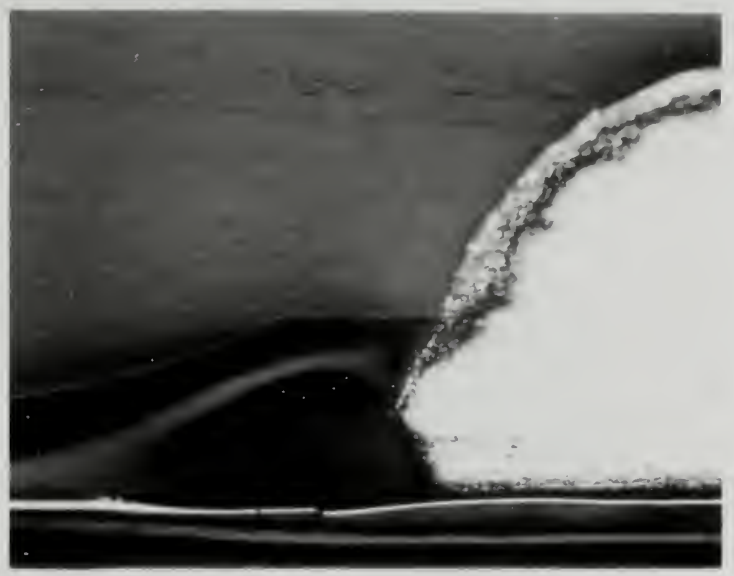

FIGURE XXVII

FIGURE XXVIII

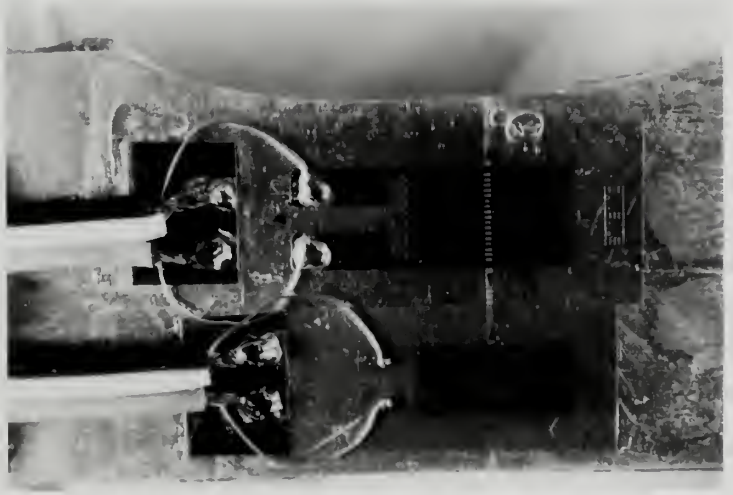

VI. DISCUSSION OF RESULTS

TEST # 1: The results of the block position calibration can best be seen in Figure III. Normally a flat prismatic cantilever specimen would show a linear plot, but the cantilever specimen used in this investigation had a reduced section which caused a slight non-linearity.

One other point should be noted. The bottom of the specimen is supported by a disk and spring arrangement. The manner in which the cantilever specimen is subjected to bending does not provide complete freedom from constraint on the free end.

Figure III is good for predicting the strain level of any specimen providing the following conditions are meet:

a) specimen has the same geometry as in Figure XXIX;

b) cantilever deflection is 0.10 inch at the point of load application;

c) strain gage is mounted on the flat side and transverse axis is located 0.0625 inch from the centerline of the reduced section toward the clamped or shorten end of the specimen;

d) the specimen is secured in the clamping block with the transverse axis of the gage 0.50 inch from the clamp.

TEST # 2: Throughout the fatigue gage investigation the strain levels were expected to range from about 2000 $\mu\epsilon$ to 5000 $\mu\epsilon$. It was desired to measure the strain of the specimen at various times during the test; however, the fatigue life of an ordinary strain gage was not known beyond 1500 $\mu\epsilon$. This test would give an indication of the fatigue life; furthermore, it would possibly show the cause of zero shift.

The strain level of this test was $\pm 3157 \mu\epsilon$ for reverse bending. When the test was stopped at 6000 cycles, a definite but small zero shift in gage resistance was noticed. At 10,000 cycles the resistance had increased even more, but was still quite small; however, between 10,000 cycles and 15,250 cycles a sharp increase occurred in gage resistance. At this point the EA strain gage was studied with a metallograph. Cracks were observed in every strand as pictured in Figure XIII and Figure XIV. Figure XIII was photographed at 100X, and Figure XIV is the same field of interest at 200X. The mean crack length at the

tip end was .00116 inch and at the base end was .00196 inch. The maximum crack length was .00315 inch or 78.8% of the width of that strand. Every crack propagated from the same area as noted in Figures XIII and XIV. It appears that the cracks are caused by stress concentrations. Since the gage was not studied at the inception of zero shift, this test did not determine whether or not cracks had developed when the zero shift occurred. Using the criteria that a strain gage is near the end of its life when zero shift occurs (29), the EA gage should not be used after 6000 cycles in this case.

TEST # 3: Initially, three gages were monitored during this test, but the EA strain gage mounted in the reduced portion of the specimen appeared to produce very little useful data. Attention was given to the S/N fatigue gage and the EA gage mounted on top of the specimen. This test was stopped as soon as a measureable zero shift occurred in the EA strain gage. A small zero shift occurred during the first 5 cycles, but this can be expected of any bonded gage (29). At 5000 cycles when the first measureable zero shift occurred, the specimen was removed from the fatigue machine and examined with a metallograph. Three small cracks were found in the gage at 5000 cycles. The specimen was again fatigued until 10,000 cycles

and removed for inspection. Zero shift of the EA strain gage had increased as well as the number and length of cracks. Hereafter, the specimen was removed and inspected each 1000 cycles in hopes of developing some useful information concerning crack length and zero shift. By inspecting the data in Appendix E, it can be observed that ΔR for the EA strain gage increases as crack length grows. Although not included in Section IV of this investigation, ΔR was plotted as a function of the mean gage crack length on log-log paper. The result was a power law relation, but due to scatter and insufficient data, the plot was not too meaningful. Also the approach of using mean gage crack length is questionable because insufficient weight is given to the longer cracks which are probably the contributing factors effecting ΔR.

In test # 2 there were 34 areas where cracks occurred. Cracks were expected in the same 34 areas in test # 3; however, five of these areas had no noticeable cracks after 17,000 cycles (ΔR of 2.04 ohms).

Two points are brought out by the crack observations. First, if a crack occurs, it will occur in the same area as noted in Figures XIII and XIV. Second, the mechanism causing small changes in resistance (i.e. 1% - 2%) of a foil gage can be attributed to cracking and not just work

hardening as assumed by Harting. It would further seem reasonable that the crack rate growth could be regulated by constraining the foil grids in an encapsulant such as used by the S/N gage.

Another purpose of this test was to compare indicated strain measurements of an EA strain gage and S/N fatigue gage. The results were plotted in Figure IV. A line was faired through the data points, but after 5000 cycles the curves need not be fair because the specimen was removed periodically and probably not replaced exactly as before. Both gages agreed extremely well for low number of cycles. In fact, in this particular test the S/N fatigue gage read almost exactly what was predicted by the calibration graph, Figure III. Over the entire range of this test the S/N gage readings showed less deviation from the value predicted by Figure III than did the EA gage. In theory, the EA gage should have given better results until a zero shift occurred. After cracks developed in the EA gage, it appears that the S/N gage gave more consistent results. As long as Rg can be determined for the fatigue gage with reasonable accuracy, strain measurements using the fatigue gage and a gage factor of 2.04 are within experimental accuracy in the low cycle range.

TEST # 4: This particular specimen was received from W. T. Bean, Inc. with a fatigue gage already mounted. The only student imput was the actual running of the test. The results were plotted in Figure V, specimen S-1. The performance curve correlated very well up to 10^4 cycles, and at that point the results deviated from the predicted. At this point no reason is given for the deviation. The gage was not studied as to be done in later tests because the specimen fractured through the gage. It was decided initially that to reduce the unknowns, any gage to be studied with a metallograph should not have been fractured.

TEST # 5: This test was similar to Test # 4 with two exceptions. The strain rate or cyclic rate was much lower in this test, 400 CPM instead of 1080 CPM. Also indicated strain readings were recorded throughout the test.

In tests # 4 and # 5 the indicated strain readings for cycles 1 and 5 were not indicative of what they should have been; hence, the next strain reading was taken as the indicated strain level for the performance curves. There are two possible reasons for this discrepancy. First, the 1018 CR steel was very rigid and therefore, the clamp was not completely rigid. Second, it was not noticed

until Test # 5 that due to spring stiffness, the spring was not causing the beam to completely deflect for 0.10 inch in compression at the top surface of the specimen.

When the ΔR data for Test # 5 was plotted as having strain range of $\pm 2500\mu\epsilon$ (actually $\pm 2497\mu\epsilon$), the correlation was excellent. No unusual phenomena were observed at the high range of cycles as noticed in Test # 4.

The second major aspect of this test is presented in Figure VI. All of the strain measurements for the fatigue gage were taken using a balanced half-bridge and a gage factor of 2.04. Two questions come to mind when viewing Figure VI. First, why does the indicated strain increase? Second, why does the tensile strain increase at a more rapid rate than the compressive strain? The answer to the first question might be approached by looking at the equation

$$\frac{\Delta R}{Rg} = \epsilon \cdot GF \qquad (4)$$

To give an increase in strain, either GF must decrease and/or $\Delta R/Rg$ increase more and more each time. Strain gage theory predicts that the strain sensitivity approaches 2.00 in the limit which would not give sufficient account for the magnitude of change noted in Figure VI. The only other reason for the increase is an increase in $\Delta R/Rg$ and is

probably due to cyclic strain-hardening of the steel which is discussed in numerous references, Manson (20) being one. Later, in Test # 10 there is a slight increase in indicated strain, but for the same zero shift the increase in indicated strain is much less.

The second question can also be approached by looking at the $\Delta R/Rg$ term of equation (4). If the material had work hardened, $\Delta R/Rg$ should not have increased any more in tension than in compression over just one-half cycle when a reading was being taken. This could have been caused by a crack in the steel specimen, but a crack did not develop until about 39,000 cycles; therefore, it would appear that cracking might have been present in the sensor for all cycles beyond at least 4000 cycles.

TESTS # 6 - # 10: These five tests were conducted on "Lucite 129" specimens. Acrylic plastic was chosen for several reasons:

a) Acrylic plastic is being used more and more in the field of Naval Architecture as transparent windows in oceanographic research ships and submarines. To date no constant strain fatigue data has been published for this material, although Marin, Pao and Cuff (21) have performed extensive creep studies.

b) Acrylic plastics fail in a brittle manner which means no cracks would be developing under an S/N fatigue gage, adding more uncertainty to this investigation.

c) Being a non-metallic there would be no magnetic phenomena induced from the fatigue specimen (29).

The performance data was plotted in Figures VII through Figure XI. The specimen fatigue life was then plotted in Figure XII. Specimens L-2 and L-3 showed excellent correlation with the predicted performance curves. Specimens L-1, L-4 and L-5 showed reasonable correlation. Specimens L-1 and L-5 departed from the predicted performance curves at high number of cycles. Specimens L-1 and L-4 appeared to oscillate about the predicted curves somewhat. No apparent reason can be given for this ocillating phenomena unless it is due to creep and relaxation in the Lucite (21).

It appears that when a gage is bonded on a Lucite specimen of the size used in this investigation, the specimen will not fail at the gage, but instead at the highest strain level just past the gage (i.e. the gage tip).

All gages which were mounted on the Lucite specimens were studied by observing longitudinal cross sections with

a metallograph. Before proceeding with discussion of these five gages, a few comments should be made concerning the observations of a gage with zero cycles. Figure XV shows a diagonal cross section of a new gage at 100X. The strands do not have a rectangular cross section, but slope to a point at the edges due to the acid etch process. The edges of the strands are not even. Numerous micro-notches exist along the edge as demonstrated in Figure XV at 100X. Figure XVI shows the notch of the middle strand in Figure XV, but magnified at 465X. Figures XVII, XVIII and XIX show the turret of the same gage. There is a small void in the lead turret. In this specimen as many as three small voids were observed in the turret at any one time. If voids exist in the lower 50% of the turret, they will be present after soldering because experience in this investigation revealed that only the upper 25% - 40% of the turret was melted during soldering when the proper connection procedures were used. Figures XVII and XVIII show the angle of the epoxy-turret interface. The angle at this interface was not consistent, but acute in some specimens and obtuse in other specimens. Figure XIX shows an acute angle of the turret in specimen L-2 after removal of the connection wire.

After studying the results from Tests # 2, # 3 and # 5, the fatigue gages were inspected for cracks. If cracks had developed, these cracks should occur in the areas of stress concentration as seen in Figures XIII and XIV for the EA strain gage. Specimen L-3, which showed excellent gage performance correlation (Figure IX), was examined first. A significant crack was found as expected in one of the places of high stress concentration (i.e. the same area as in the EA strain gage). This crack was located at the base end of the third strand, numbering from the outer most strand. At the very outside edge of the strand, the crack had opened approximately 2 - 3 mils. In one portion of the strand adjacent to the crack, a very small void had been created. It is unfortunate that in the process of polishing for a clear photograph at 1000X this area of interest was lost; however, after polishing the area to a depth of 9.84×10^{-4} inch, Figure XX was obtained at 1000X*. The average strand thickness is 2 mils which can be used as a scale in the photograph. If this crack had been viewed looking down at the strand, the actual reduction

---

* It was not possible to get a clear picture at 1000X unless an oil lens was used. No oil lens was available at the time of photographing.

in area at this section could not have been determined because there were different reductions above and below the strand. Cracks were found in other gages, but not all strands contained cracks..

As mentioned previously the outside edges of each strand were very uneven. Figures XXI and XXII taken at 1000X of specimen L-1 and L-5 respectively demonstrate this point. The average strand thickness at mid-section is 2 mils. The maximum thickness in Figures XXI and XXII is approximately 1 mil.

Figure XXIII taken at 500X, shows one of the areas of specimen L-5 where a crack might be expected to develop. The thick portion in the right of the photograph is the end of the strand, and the thin portion is the edge of a strand which is joining at the inside radius. Figure XXIV, taken at 500X, shows the same area after a very brief polishing (approximately .001 mm). The small cracks in these two photographs are probably notches due to etching and not really cracks. There are several pits in the strand which were never noticed in a gage which had not been fatigued. The reason for these pits is unknown, although it is possible that the pits are caused by work hardening.

Specimen L-5 did not exhibit good correlation at the higher cycle range. It is believed that a large void next

to the turret helped contribute to this phenomena. The void is shown in Figure XXV at 100X and Figure XXVI at 200X. The photographs show a crack in the foil grid below the void. The crack could have developed during polishing because the foil was not rigidly constrained at that point. The cause for the crack cannot be readily ascertained, but the crack is long enough that it could not be polished out. It probably extended across the void. A combination of the crack and possible non-rigidity of the turret to the foil could have caused a rapid increase of ΔR.

Other phenomena were noticed that could cause an unexpected increase in the slope of $\Delta R/N$. Specimen L-4 had a rather large void in the lead turret which may have contributed to the ocillating effect in the performance curve. If the life of the specimen had been longer, a permanent ΔR deviation may have been noticed. If voids exist in the lead turret, they could certainly cause unpredictable effects as the void geometry changes due to cold working.

Poor solder connections to the turret or excessive melting of the turret might give erratic results in $\Delta R/N$. No difficulty was experienced in this investigation with connections failing as noted by Horne (17).

Cracking of the grid can not be ruled out as causing the unexpected increase in $\Delta R/N$. This deviation phenomenon occurs after many cycles of fatigue and one crack sufficiently well propagated could certainly cause an unexpected increase of $\Delta R/N$.

Most of these tests were run at different cyclic rates in an attempt to determine if strain rate effected the fatigue gage performance. No definite conclusions were reached.

Several times while taking data it appeared that ΔR increased slightly with time with the beam at no load. Specimen L-5 definitely exhibited this tendency as can be seen in the data for Test # 10, Appendix E. This is contrary to Horne's results in which he cites a decrease in ΔR with time. One might expect a decrease in ΔR due to possible relaxation of the specimen. To give an increasing ΔR, a crack would have to be propagating in the specimen or the fatigue gage. The Lucite specimen would not support crack propagation without complete fracture. This leaves the possibility of gage cracking.

TEST # 11: The data used in this test was from a very small sample field, only two specimens. Using Triebes' (31) specimens two fatigue gages were checked for any long time effects on change of resistance. ΔR of one gage had

increased by 29.7% and the other by 48.5% over a 12 month period. Since the gages were still securely bonded, this leaves the possibility of stress-corrosion in the aluminum specimen or the fatigue gage or both. No cracks could be seen in the aluminum. Swann (28) mentions stress-corrosion in some copper alloys if ammonium ions are present. The exact production process used in manufacturing of the S/N fatigue gage is not known, but some photo etching processes definitely have ammonium ions present (8, 27). If any trace of ammonium ions were present after a manufacturing process, the fatigue gage could possibly be effected by stress-corrosion.

VII. CONCLUSIONS

The S/N Fatigue Gage was designed to predict fatigue failures before a catastrophic failure occurs. This is accomplished by comparing the data with performance curves such as Figure I and correlating ΔR with the per cent life remaining in the material subjected to fatigue. Under ideal test conditions this investigation did, in general, show that the performance curves are reproducible.

The mechanism by which the fatigue gage operates is not due to cold working alone. Cracking of the foil material contributes to the resistance change of the gage. It is possible that cracking may be the contributing factor after several thousand cycles, depending upon the strain range. Cracking can contribute to small changes in resistance (1% - 2%) and is not restricted to large resistance changes. If cracking occurs, the cracks can be found at either ends of the strands where the inside radius joins the strand.

The S/N fatigue gage can be used as a strain gage with reasonable accuracy; however, for the higher cycle range there is a more rapid increase in indicated tensile strain than compressive strain. The compressive strain should give a more accurate indication of strain level.

There is indication that voids in the epoxy, adjacent to the turrets and voids in the lead turrets may cause deviation from the predicted performance curves at higher cycles of fatigue. Cracking of the foil grid may also be a possibility contributing to this deviation, if the cracking occurs erratically. No cracking occurred in any of the terminal hook up wires in this investigation. Figures XXVIII and XXX show the type of hook up used and was very successful.

No definite conclusion was reached concerning gage performance as a function of cyclic bending rate.

This investigation showed that for short time tests on Lucite, resistance change increased slightly as a function of time. For one long time test on aluminum, resistance change increased as a function of time, probably due to stress corrosion in the aluminum or possibly, in the gage depending upon the manufacturing process.

The strands of the fatigue gage do not have a rectangular cross section, but taper toward the edge in a somewhat ogival fashion. There are numerous micronotches along the edge of the strands and the strand thickness varies greatly along the edges.

The procedures for mounting the gages (Appendix A.)

were very successful. The procedure of cleaning the back of the fatigue gage with ammonia neutralizer is questionable. If constantan is susceptible to stress-corrosion when exposed to ammonia, it is possible that during lapping the back of the gage with pumice, a path could be opened to the foil via one or several of the voids in the epoxy through which ammonia might flow.

When the fatigue gage is mounted on Lucite, the specimen will not fail at the gage but at some point just past the gage. It appears from Figure XII that "Lucite 129" will have a long fatigue life below strain levels of 1900$\mu\varepsilon$.

VIII. RECOMMENDATIONS

The ideal investigation of the S/N fatigue gage would include examining the surface and the cross section of the gage. The following procedure is recommended for a more thorough investigation of the type initially attempted in this paper:

a. Find an adequate solvent for removing the epoxy from the gage surface;

b. Examine the foil surface with a scanning electron microscope;

c. Examine the gage cross section by first etectro-plating with nickel, then mounting the gage for polishing. This would protect the edges of the foil from any possible cold flow while polishing;

d. Attempt to determine the change in resistivity as a function of cold working.

Additional tests should be conducted to determine the effect of change in gage resistance as a function of time.

Wood (34) recommends conducting constant strain fatigue tests on cylindrical samples. It would be interesting to conduct tests with the fatigue gage mounted on cylindrical

specimens and compare the results with results obtained from flat specimens.

The plot of strain versus cycles for "Lucite 129" (Figure XII) should be supported by additional data. More specimens should be tested to confirm the shape of the curve.

IX. APPENDIX

A. PREPARATION OF BENDING SPECIMENS

After considering several geometrical configurations, the W. T. Bean standard S/N fatigue specimen was chosen as a desireable geometric shape. A specimen of the geometry shown in Figure XXIX was chosen for the following reasons:

1. the specimen as designed for the W. T. Bean portable S/N fatigue machine, although the specimen had to be shortened 0.50 inch to permit its use in clamping block position # 3; (See Appendix C for a detailed description of the portable S/N fatigue machine.);

2. the specimen would eliminate one parameter (i.e. different geometry) which might cause deviation from the manufacturer's predicted gage performance;

3. the geometry was such as to induce fracture at the same local area during each test;

4. the specimen was appropriately sized to mount one S/N fatigue gage at the reduced section of the specimen;

FIGURE XXIX

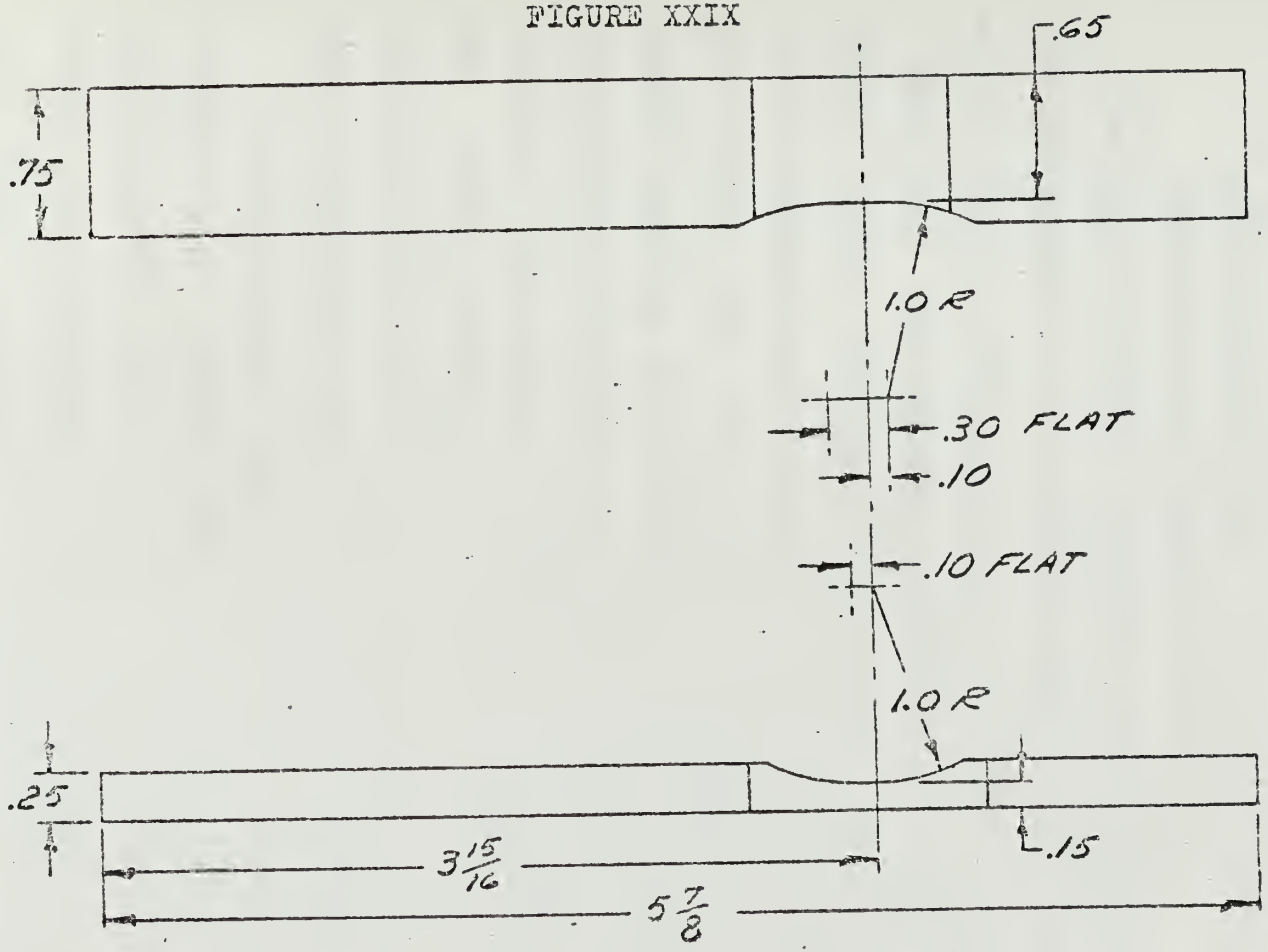

-S/N- FATIGUE SPECIMEN - PLAIN

10-1-66

DESIGNED BY W. T. BEAN

DRAWN H. J. J.

5. the specimen required a limited amount of material and could be machined from standard stock materials by the student in the M.I.T. student machine shop.

The reverse bending specimens were fabricated from cold rolled 1018 steel, 2024-T4 aluminum and "Lucite 129" acrylic plastic. The steel specimens were donated by W. T. Bean, Inc. The aluminum specimens were machined from 0.750" x 0.250", 2024-T4 aluminum stock. The acrylic plastic specimens were cut and machined from 0.250" cast sheet "Lucite 129". In addition to machining, the acrylic plastic specimens were annealed at 160°F for 4 hours. All machining was performed along the longitudinal axis of each specimen. There were no machine marks along the transverse axis. After machining, all specimens were polished with very fine emery cloth. In the case of the plastic specimens the polishing was performed before annealing.

One S/N fatigue gage was mounted on the flat surface of each fatigue specimen with the gage centerline at a distance of 0.062" from the center of the reduced section and towards the clamped end. Prior to mounting each gage, standard surface preparation procedures were followed. The entire procedure was as follows:

1) insure temperature of specimen at or slightly above 70°F;

2) lap surface with silicon carbide paper dipped in Bean metal conditioner (240 grit for steel and aluminum; 400 grit for plastic); remove residue with clean tissue;

3) repeat step b) and mark gage location with 6 H pencil;

4) apply metal conditioner to surface with cotton swab and remove with one stroke of clean tissue;

5) apply ammonia neutralizer to surface with cotton swab and remove with one stroke of clean tissue;

6) using fine pumice powder, lap bonding surface of gage and teflon terminal strip with a circular motion on clean glass plate, using finger to apply light uniform pressure to top surface of gage and terminal strip;

7) place gage face up on clean glass surface and position terminal strip directly against the end of gage;

8) apply cellophane tape over top of gage and terminal strip;

9) lift gage and terminal slowly from glass surface and clean back with cotton applicator dampened with ammonia neutralizer;

10) place gage in position of specimen which was marked

previously with a 6 H pencil;

11) starting at one end of cellophane tape lift gage assembly, leaving the other end firmly attached to the specimen;

12) apply thin film of blue Eastman 910 catalyst to back of gage and terminal strip and allow to dry for approximately 1 minute;

13) apply two drops of Eastman 910 adhesive to gage area of specimen. If adhesive has been stored in refrigerator, allow it to reach room temperature before using;

14) feed gage and tape onto surface, holding free end of tape above surface with one hand and using ball of tissue in other hand to quickly force gage assembly into place with one stroke;

15) within one second press gage firmly into contact with surface using a small teflon sheet while applying pressure with a finger for thirty seconds;

16) after approximately two minutes the cellophane tape was removed;

The solder turrets of the S/N fatigue gage are 1.5% silver, 5% tin and 93.5% lead. The turrets melt at 585°F, and if this occurs, the lead will flow onto the soldering iron, thus ruining the gage. No solder connection can then

be made to the gage. The next few steps are therefore, most important.

17) set powerstat voltage at 95 VAC for a 22.5 watt soldering iron with a .125 inch chisel point tip;
18) tin terminal strip and gage solder turrets with rosen core 63-37 tin-lead (Bean 300°F) solder;
19) remove approximately .50 inch of the insulation from the end of a stranded # 30 copper lead;
20) separate a single strand from the rest; solder the others together and cut the soldered group to approximately .125 inch length;
21) tape leads to specimen surface and solder to terminal strip;
22) form the single strand to a "C" shape so that the free end lays on top of the turret. Anchor the loop using masking or cellophane tape so that the loop end is firm against the solder turret;
23) lay the rosin-cored solder on top of the solder junction and bring soldering iron down on joint; remove solder and then lift iron;
24) float tape loose with rosin solvent and remove all solder flux.

FIGURE XXX

S/N FATIGUE GAGE AND TERMINAL

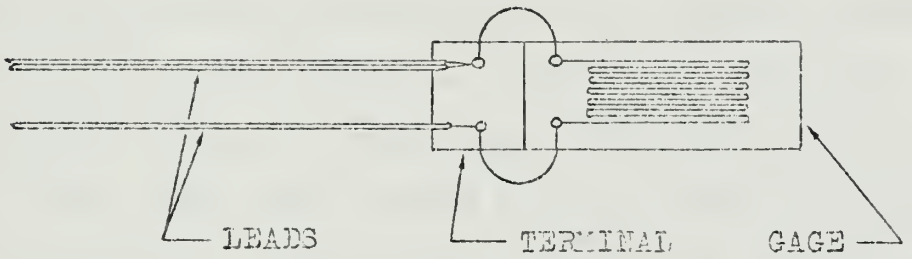

Several points in the S/N installation are worth reiterating which will improve test results and reduce scatter when tests are reproduced.

a) Insure that soldering iron temperature is not raised much above 300°F. High temperatures will damage the solder turrets on the gage.

b) Position terminal strip directly against gage and use a "C" shape in the single strand connection. This will minimize fatigue failure in the electrical connection.

c) If the installation will permit, position terminal strip in the lower strain field and lead the electrical connections away from the higher strain field in the direction of the lower strain field.

Two aluminum specimens were subjected to fatigue with Micro-Measurement Type EA strain gages. These gages were mounted similar to the above procedures except there were no solder turrets and lapping was not necessary.

B. PREPARATION OF METALLOGRAPH SPECIMENS

The S/N gages were removed from the fatigue bending specimens using epoxy stripper. The Eastman 910 epoxy bond is easily broken with any epoxy stripper listed in TABLE I. The gages were mounted in Bansel "E-Z" Plastic Mount for polishing. The maximum temperature during setting was about 135°F. To observe the microstructure of a metal, a flat, mirrorlike surface must first be polished on the sample. Polishing for structural observations requires the attainment, or approximation of a mirrorlike surface by cutting away normal irregularities rather than by causing high areas to flow into low areas, as in buffing.

All specimens were polished on three successive rotating disks. The first step used a disk covered with a 600 grit abrasive. The second step incorporated a special cloth (Buehler microcloth), mounted on a disk which was periodically saturated with an abrasive solution consisting of 2 tablespoons of 0.3 micron alumina powder in one pint of distilled water. The third polishing step incorporated a special cloth on a separate disk from step 2, and an abrasive solution of 2 tablespoons of 0.05 micron alumina powder in one pint of distilled water. The only means of inspecting the progress of the polishing process

was to view the specimen through an optical microscope at 500X.

The entire polishing process is rather difficult and time consuming for specimens as small as a strain gage before a satisfactory surface is obtained for photographing. It is extremely important to periodically clean the polishing wheels with distilled water to prevent build up of any large particles on the polishing cloth.

Many etchants were tried in order to bring out the grain structure of the gage, but no satisfactory etchant was found to properly etch the small cross section. Since the specimens were not etched, any etch like appearance at the edges of the fatigue gage strands are the results of the gage manufacturing process.

C. DESCRIPTION OF APPARATUS

S/N FATIGUE MACHINE

All fatigue tests were run on the W. T. Bean S/N fatigue machine as shown in Figure XXXI. This machine was chosen so that the possibility of deviation between the manufacturer's predicted gage performance and results of this experiment might be minimized.

The machine is quite small and therefore, portable. It is a constant displacement device for low cycle (i.e. less than 10^4 or 10^5 cycles) fatigue studies of a cantilever beam in bending. The machine can provide reverse bending, all tension or all compression depending upon the desires of the operator; furthermore, the machine permits subjecting the bending specimen to a number of different strain levels although this range is limited in reverse bending to approximately 2000$\mu\epsilon$ - 5000$\mu\epsilon$.

The operation of the machine is quite simple. A variable speed motor drives a fly wheel to which is attached a ball bearing eccentric. The eccentric rests on one side of the cantilever and a spring loaded disc rests on the opposite side of the beam. The eccentricity is 0.2 inch, thereby giving a maximum displacement of 0.2 inch for pure compression or pure tension and $\pm$ 0.1 inch

FIGURE XXXI

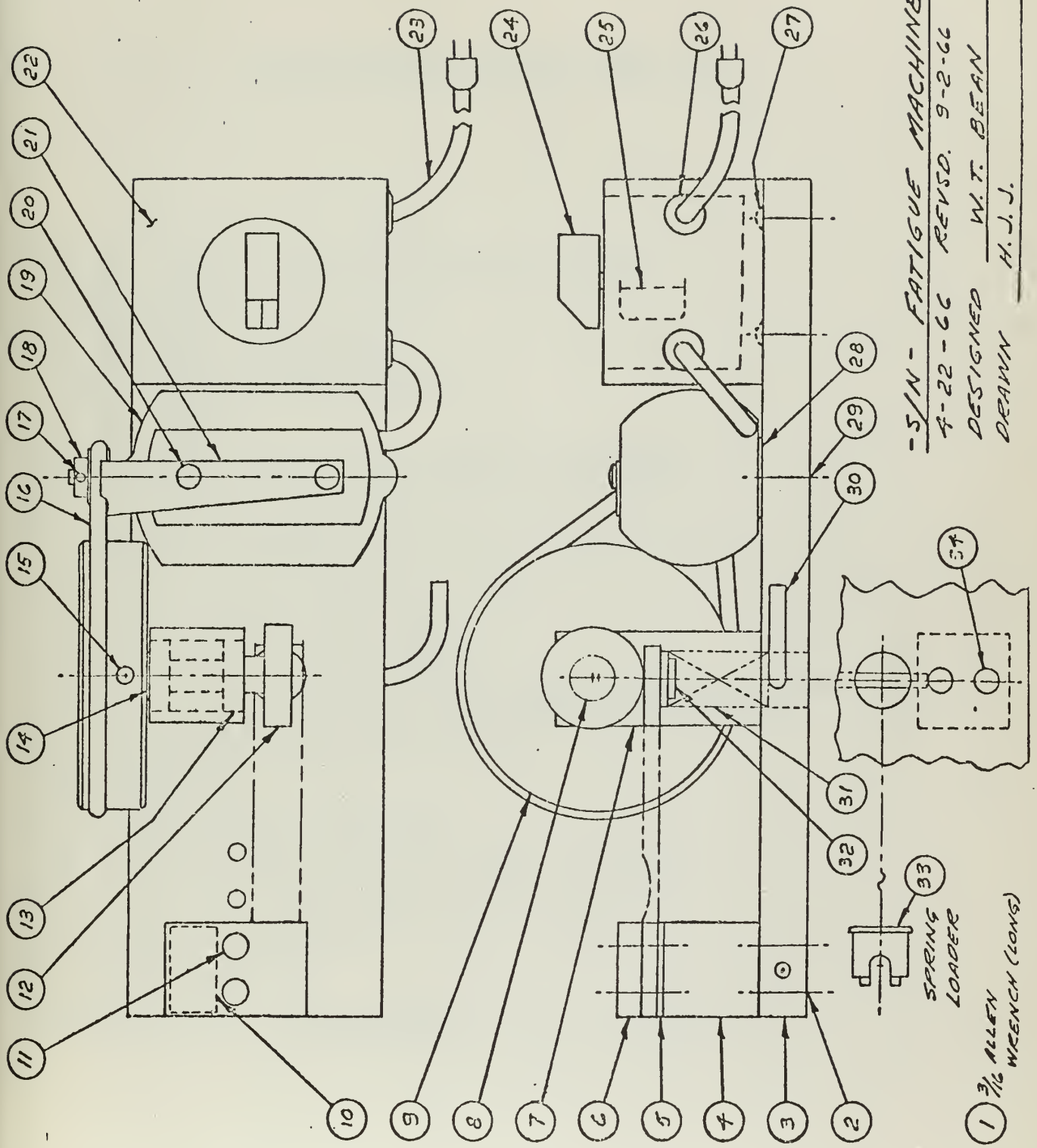

188.1

-S/N- FATIGUE MACHINE PARTS LIST

(1) 3/16 Allen wrench (long)
(2) 1/4 - 20 x 1 Allen cap screws (2 req.)
(3) Base plate
(4) Specimen clamping block
(5) Specimen shim plate
(6) Specimen clamping plate
(7) Cam shaft bearing housing
(8) Cam shaft
(9) Fly-wheel
(10) Specimen compensating block for clamping
(11) 1/4 - 20 x 1 Allen cap screws (2 req.)
(12) Cam bearing (ND 77R12)
(13) Cam shaft support bearings (ND 77R8) (2 req.)
(14) 1/2 inch flat washer
(15) 1/4 - 28 x 1/4 Allen set screw
(16) Vacuum cleaner belt #105
(17) 8 - 32 x 1/4 Allen set screw
(18) 3/4 inch dia. drive pulley
(19) Drive motor, Dayton Electric Mfg. Co., Model 2M037 1/10 hp.
(20) 10 - 32 x 1/4 Philips round head screw (2 req.)
(21) Belt damper plate (adjustable)
(22) 115 VAC power cord
(23) Powerstat
(24) 600VDC, .01 MF capacitor
(25) Cord grommets (2 req.)
(26) 8 - 32 x 1/2 round head screws (3 req.)
(27) 0.062 inch thick shims
(28) 10 - 32 x 1 flat head screws (2 req.)
(29) Spring retainer pin
(30) Loading spring
(31) Spring cap
(32) Spring installation plug
(33) 1/4 - 20 x 1-1/4 Allen cap screws (2 req.)

for reverse bending. For reverse bending the fixed end of the cantilever beam is placed in a clamping block with a 0.1 inch shim plate on top of the beam. The clamping block may be located in three standard positions depending upon the desired strain level. A fourth non-standard position can be provided if a longer specimen is used, and only one set screw is used to hold the clamping block in position.

In order to determine the fly-wheel speed a strobe light or fluorescent lamp must be focused on a white diametrical line located on the fly-wheel. By obtaining the proper image the fly-wheel speed is obtained. Knowing the fly-wheel speed and having a stop watch, the number of cycles can be determined. The fly-wheel must be turned manually to keep accurate count of the first few cycles.

The above method of determining the number of cycles was not used. The machine was modified slightly by building a counting mechanism which consisted of a 110 volt, 60 cycle electric counter in series with a micro-switch. The micro-switch was actuated by the eccentric. For each revolution of the eccentric the micro-switch closed once and the counter recorded one count. The counter was a 6 digit counter.

S/N RESISTANCE METER

The W. T. Bean S/N RESISTANCE METER is a null-balance, Wheatstone Bridge type instrument specifically designed to measure resistance or resistance increase (ΔR) in S/N Fatigue Life gages. The measurement range is from 100 to 200 ohms. The value of ΔR above 100 ohms is read directly on a three-digit dial in units of 10's, 1's and 1/10's. The meter is designed to receive three-wire imput for eliminating lead-in wire resistance from the measurement. The meter has a high and low sensitivity button so that the meter can be quickly nulled. Once the meter is nulled by observing a needle on a galvanometer the value of ΔR can be easily read from the digital nulling dial. Battery voltage effects the sensitivity of the meter, but does not effect the value of ΔR.

STRAINSERT STRAIN INDICATOR

The Strainsert, Model HW-1, was used to measure small resistance changes (ΔR) below 100 cycles and strain level of the S/N gage or EA strain gage. The instrument is designed for use with Wheatstone full-bridge or half-bridge strain gage circuits. It is calibrated to read directly in micro-inches per inch strain when used with strain gages having resistances between 50 and 2,000 ohms and gage factors between 1.50 and 4.50. The instrument can be read to an accuracy of about 2$\mu\varepsilon$.

METALLOGRAPH

The Metallograph, manufactured by the American Optical Company, is a versatile device which permits magnified optical viewing, micro measuring, and photographing that part of the specimen in the field of vision. The specimen can be easily translated in any direction with micrometer knobs to permit rapid viewing of any part of the specimen. Normal use of the optics permits magnification of 100X, 200X, 500X and 1000X. Additional magnification of 50X, 75X and 1,500X can be obtained with special adapters or accessories.

The optical system permits viewing the specimen through eye pieces or a projected image on a camera adapter. The camera adapter receives a Polaroid Land Camera for photographic work. The adapter has a wide range of shutter speeds. The proper exposure is determined by an appropriate adjustment of the illumination intensity knob and shutter speed.

S/N FATIGUE LIFE GAGES

The S/N fatigue gages have a constantan foil* (copper-

---

* Specific details of the foil are proprietary; however, since the gage is designed to work harden a logical conclusion would be that the foil is an annealed foil rather than ¼ or ½ hardened foil.

nickel alloy also known as Advance, Cupron, and Copel) grid. The constantan grid is completely encapsulated (24) in a high-functionality epoxy resin system which is reinforced with glass fibers on both sides of the gage. Connections are made to solder turrets which are mechanically bonded to the grid foil and held firmly in place by the epoxy system. The following data applies to the S/N gages used:

Manfacturer: Micro-Measurements, Inc.

Type: NA-01

Resistance: 100.0 ± .2% ohms

Nominal Gage Factor: 2.04

Lot Numbers: A12AP15, Z-A12AP21

EA STRAIN GAGES

The EA strain gages are open-face gages having a constantan foil grid and a general purpose epoxy backing which is tough and flexible. (24). The following information applies to the strain gages used:

Manufacturer: Micro-Measurements, Inc.

Type: EA-13-250BB-120

Resistance: 120.0 ± .2 ohms

Gage factor: 2.095 ± .5%

Lot Number: A14AF46

Fatigue Life: 10^6 cycles @ ± 1000 $\mu\epsilon$
10^5 cycles @ ± 1500 $\mu\epsilon$

D. SAMPLE CALCULATIONS

Strain Calibration

All test specimens were cantilever beams with constant alternating displacement. Assume the beam is a weightless,

FIGURE XXXII

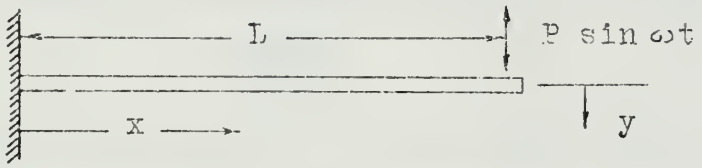

prismatic beam as shown in Figure XXXII. Solving for the maximum deflection knowing the maximum instantaneous bending moment:*

$$E\ I\ y'' = \pm M = \pm P(L-x) \qquad (5)$$

Integrating once,

$$E\ I\ y' = \pm\left[PLx - \tfrac{1}{2}Px^2 + C_1\right] \qquad (6)$$

but $y' = 0$ when $x = 0$, therefore $C_1 = 0$;

Integrating again,

$$E\ I\ y = \pm\left[\tfrac{1}{2}PLx^2 - \tfrac{1}{6}Px^3 + C_2\right] \qquad (7)$$

but $y = 0$ when $x = 0$, therefore $C_2 = 0$;

---

* Ebner and Backofen (11) found for alternating bending, constant deflection tests with strain amplitude of approximately .2% that the bending moment was not constant, but increased slightly between 10^2 - 10^3 cycles for metallic specimens.

When x= the value of y at the free end is found to be;

$$y = \pm \frac{PL^3}{3EI} \tag{8}$$

Since these tests were run at constant displacement or deflection, equation (8) can be rearranged to yield;

$$P = \pm \frac{3EIy}{L^3} \tag{9}$$

The elastic strain at the outer fiber of the beam is:

$$\epsilon = \frac{Mc}{EI} \tag{10}$$

Now, combining equation (5), (9) and (10) yields

$$\epsilon = \pm \frac{3EIy}{L^3} \cdot (L-x) \cdot \frac{c}{EI} \tag{11a}$$

$$\epsilon = \frac{3y(L-x)c}{L^3} \tag{11b}$$

From equation (11b) it can be seen that for a constant deflection cantilever beam test, the strain at a given distance x is a function of geometry and independent of material tested. Even though the test specimens were not exactly prismatic, the conclusions would be the same and the value of strain would differ slightly from equation (11b).

Since the test specimens were rather small for mounting fatigue and strain gages and strain gages have short fatigue life at high strain, only the fatigue gages were mounted; however, a strain gage was mounted on one piece of aluminum (2024-T4) and strain measurements taken with clamping block in positions 1, 2 and 3. The strain calibration results are tabulated in Table II.

TABLE II

STRAIN CALIBRATION

Function	Units	Block Position* 1	2	3
x	inches	0.50	0.50	0.50
y	inches	0.10	0.10	0.10
L	inches	3.90	3.15	2.40
ϵ_c	$\mu\epsilon$	-2400	-3165	-4480
ϵ_t	$\mu\epsilon$	+2360	+3150	+4610
ϵ_T	$\mu\epsilon$	4760	6315	9090
ϵ_R	$\mu\epsilon$	$\mp$2380	$\mp$3157	$\mp$4545

Computation of Small ΔR

For large values of N and ΔR the Bean S/N Resistance Meter was used; however for values of ΔR below N= 100 cycles more accuracy can be obtained by using a strain indicator. Before commencing a run the strain indicator was hooked up as a Wheatstone half-bridge with Rg in one leg and a dummy value of Rg in the other leg. The bridge was nulled with the strain indicator after the nominal gage factor (2.04) was set on the gage factor dial. Since for small values of ΔR, Rg is essentially constant, and the following equation can be used to compute ΔR:

---

* The block can be placed in a position such that L= 4.65 inches, but the test specimen must be longer than the specimen for the other position. No calibration was run with the block in this position. Also the strain can be varied slightly by varying x somewhat, but this is limited by specimen geometry.

$$\Delta R = (\Delta \epsilon) \cdot Rg \cdot GF \qquad (12)$$

If Rg = 100 ohm and GF = 2.04, this becomes

$$\Delta R = 204(\Delta \epsilon) \qquad (13)$$

where $\Delta \epsilon$ is expressed in inch per inch. Equation (12) can also be used to compute ΔR for N>100 cycles if Rg is increased by ΔR during each measurement and this value is substituted as the dummy resistance in the half-bridge. During each interval of N, Rg in equation (12) would be up dated. The total ΔR over a large value of N would then be the summation of all the incremental values of ΔR.

E. TABULATION OF DATA

TEST # 1: Clamping Block Position Calibration for Reverse Bending

Material: Aluminum 2024-T4

Design: Flat Bar

Serial No.: A-1

Strain Indicator: Strainsert HW-1

Gage Type: EA - 13 - 205BB - 120

Type Loading: Reverse Bending

Block Position	ϵ_c*	ϵ_t	ϵ_T	ϵ_R	x	y	L
1	-2400	2360	4760	±2380	0.50"	0.10"	3.90"
2	-3165	3150	6315	±3157	0.50"	0.10"	3.15"
3	-4480	4610	9090	±4545	0.50"	0.10"	2.40"

* All strain measurements in Tabulation of Data will be given in microstrain.

TEST # 2: Zero Shift of EA Strain Gage

Material: Aluminum 2024-T4

Design: Flat Bar

Serial No.: A-2

Strain Indicator: None (S/N Resistance Meter)

Gage Type: EA - 13 - 205BB - 120

Clamping Block Position: # 2 ($\epsilon_R = \pm 3157$)

Type Loading: Reverse Bending

N	Rg	
0	119.80	
1000	119.80	
6000	119.95	
10,000	120.15	
15,000	143.00	Test Terminated

Strand	Crack length (inch) Base	Tip
outside	-	.00060
1	.00125	.00180
2	.00200	.00020
3	.00170	.00123
4	.00250	.00115
5	.00135	.00120
6	.00260	.00130
7	.00185	.00170
8	.00315	.00145
9	.00280	.00150
10	.00200	.00125
11	.00160	.00195
12	.00140	.00030
13	.00165	.00125
14	.00225	.00050
15	.00170	.00140
16	.00250	.00090
outside	-	.00120

TEST # 3: EA Strain Gage and S/N Fatigue Gage Comparison of Zero Shift and Indicated Strain

Material: Aluminum 2024-T4

Design: Flat Bar

Serial No.: A-3

Strain Indicator: Strainsert HW-1

Gage Types: EA - 13 - 205BB - 120

NA - 01

Clamping Block Position: # 2

Type Loading: Reverse Bending

Cycle No.	Gage	Rg	ϵ_c	ϵ_t	ϵ_T	ϵ_a
0	Top EA	120.50				
0	Bottom EA	119.80				
0	Top S/N	100.15				
0	Dummy EA	120.32				
1	Top S/N	100.35	-3155	3200	6355	±3177
2	Top EA	120.50	-3200	3225	6425	±3212
3	Bottom EA	119.80	-3300	3287	6587	±3293
5	Top S/N	100.45	-3173	3207	6380	±3190
6	Top EA	120.56	-3220	3233	6453	±3226
7	Bot EA	119.90	-3207	3173	6380	±3190
10	Top S/N	100.49	-3170	3155	6325	±3162
11	Top EA	120.57	-3220	3240	6460	±3230
12	Bot EA	119.92	-3285	3315	6600	±3300
500	Top S/N	101.30	-3210	3170	6380	±3190
501	Top EA	120.56	-3210	3220	6430	±3215
502	Bot EA	119.92	-3310	3300	6610	±3305
1000	Top S/N	102.00	-3193	3210	6403	±3201
1001	Top EA	120.56	-3200	3240	6440	±3220
1002	Bot EA	119.92	-3335	3290	6625	±3312

TEST # 3: (Continued)

5000	Top S/N	104.25	-3235	3233	6468	±3234
5001	Top EA	120.53	-3195	3245	6440	±3220
5002	Bot EA	119.99	-3500	3310	6810	±3405

Specimen removed for metallograph inspection.

10,000	Top S/N	105.26	-3190	3240	6430	±3215
10,001	Top EA	120.80	-3120	3245	6365	±3182
10,002	Bot EA	120.56	-4055	3360	7415	±3707

Specimen removed for metallograph inspection after each 1000 cycles

11,000	Top S/N	105.30	-3210	3260	6470	±3235
11,001	Top EA	120.91	-3155	3210	6365	±3182
11,002	Bot EA	120.60	-3670	3990	7660	±3830
12,000	Top S/N	105.36	-3150	3215	6365	±3182
12,001	Top EA	121.00	-3080	3210	6290	±3145
12,002	Bot EA	Readings discontinued				
13,000	Top S/N	105.40	-3090	3240	6330	±3165
13,001	Top EA	121.29	-3040	3180	6220	±3110
14,000	Top S/N	105.56	-3140	3180	6320	±3160
14,001	Top EA	121.48	-3030	3180	6210	±3105
15,000	Top S/N	105.70	-3080	3190	6270	±3135
15,001	Top EA	121.78	-3100	3220	6320	±3160
16,000	Top S/N	105.79	-2940	3265	6205	±3102
16,001	Top EA	122.20	-2970	3260	6230	±3115
17,000	Top S/N	105.83	-3140	3190	6330	±3165
17,001	Top EA	122.60	-3205	3250	6455	±3227

TEST # 3: (Continued)

Crack length data:

Strand	N = 10,000 Crack length (in.) Base	Tip	N = 11,000 Crack length (in.) Base	Tip
outside	-	.00000	-	.00000
1	.00100	.00070	.00150	.00105
2	.00000	.00000	.00035	.00000
3	.00080	.00000	.00085	.00065
4	.00090	.00000	.00125	.00000
5	.00000	.00050	.00050	.00080
6	.00000	.00000	.00080	.00000
7	.00000	.00100	.00000	.00145
8	.00000	.00000	.00000	.00035
9	.00100	.00000	.00120	.00045
10	.00050	.00050	.00110	.00000
11	.00000	.00000	.00060	.00075
12	.00000	.00000	.00040	.00000
13	.00060	.00000	.00080	.00055
14	.00060	.00000	.00085	.00010
15	.00100	.00000	.00120	.00055
16	.00000	.00000	.00080	.00000
outside	-	.00000	-	.00045

Strand	N = 12,000 Crack length (in.) Base	Tip	N = 13,000 Crack length (in.) Base	Tip
outside	-	.00000	-	.00000
1	.00175	.00120	.00200	.00160
2	.00050	.00000	.00070	.00000
3	.00100	.00100	.00125	.00120
4	.00130	.00000	.00165	.00000
5	.00060	.00100	.00090	.00110
6	.00105	.00000	.00120	.00000
7	.00000	.00150	.00020	.00175
8	.00030	.00040	.00070	.00050
9	.00140	.00050	.00165	.00060
10	.00135	.00000	.00150	.00000
11	.00060	.00100	.00090	.00120
12	.00050	.00000	.00060	.00000
13	.00100	.00070	.00120	.00100
14	.00100	.00020	.00130	.00040
15	.00125	.00070	.00150	.00080
16	.00105	.00020	.00120	.00020
outside	-	.00060	-	.00075

TEST # 3: (Continued)

Crack length data:

Strand	N = 14,000 Crack length (in.) Base	Tip	N = 15,000 Crack length (in.) Base	Tip
outside	-	.00000	-	.00000
1	.00230	.00180	.00255	.00210
2	.00090	.00000	.00105	.00000
3	.00145	.00160	.00160	.00190
4	.00180	.00000	.00200	.00000
5	.00100	.00140	.00120	.00160
6	.00140	.00000	.00160	.00000
7	.00040	.00220	.00050	.00250
8	.00080	.00080	.00110	.00100
9	.00190	.00090	.00200	.00120
10	.00180	.00000	.00190	.00000
11	.00120	.00140	.00140	.00160
12	.00120	.00000	.00135	.00030
13	.00140	.00120	.00180	.00140
14	.00160	.00060	.00170	.00085
15	.00170	.00120	.00210	.00150
16	.00106	.00020	.00125	.00040
outside	-	.00090	-	.00110

Strand	N = 16,000 Crack length (in.) Base	Tip	N = 17,000 Crack length (in.) Base	Tip
outside	-	.00000	-	.00000
1	.00275	.00230	.00300	.00260
2	.00140	.00000	.00150	.00000
3	.00180	.00210	.00200	.00230
4	.00230	.00000	.00250	.00000
5	.00140	.00180	.00160	.00210
6	.00180	.00000	.00200	.00000
7	.00070	.00290	.00100	.00310
8	.00140	.00110	.00150	.00130
9	.00250	.00130	.00265	.00150
10	.00230	.00000	.00240	.00000
11	.00180	.00190	.00200	.00200
12	.00150	.00060	.00180	.00080
13	.00190	.00170	.00230	.00185
14	.00200	.00100	.00230	.00120
15	.00230	.00180	.00270	.00200
16	.00170	.00050	.00220	.00060
outside	-	.00120	-	.00150

TEST # 4: S/N Fatigue Data

Material: 1018 CR Steel

Design: Flat Bar

Serial No.: S-1

Strain Indicator: Strainsert HW-1

Gage Type: HA-01 Lot: Z-A12AP21 (ASSUMED)

Gage Factor Setting: 2.04

Clamping Block Position: # 1

Temperature: 71°F

Type Loading: Reverse Bending

Bending Rate: 1080 CPM

Cycle No.	ϵ_c	ϵ_t	ϵ_T	ϵ_R
1	-2065	2480	4545	±2273
5	-2045	2510	4555	±2277
1000	-2140	2730	4870	±2435

Cycles	Rg	ΔR
0	100.3	0.0
1	100.3	0.0
5	100.3	0.0
1,000	101.0	0.7
3,000	101.7	1.4
6,000	102.4	2.1
10,000	103.1	2.8
15,000	103.9	3.6
20,000	104.4	4.1
25,000	104.6	4.3
30,000	104.9	4.6
35,000	105.14	4.84
40,000	105.3	5.0
50,000	FAILED	

TEST # 5: S/N Fatigue Data

Material: 1018 CR Steel

Design: Flat Bar

Serial No.: S-2

Strain Indicator: Strainsert HW-1

Gage Type: NA-01 Lot: Z-A12AP21

Gage Factor Setting: 2.04

Clamp Block Position: # 1

Temperature: 71°F

Type Loading: Reverse Bending

Bending Rate: 400 CPM

Cycle No.	ϵ_c	ϵ_t	ϵ_T	ϵ_R
1	-2257	2243	4500	±2250
5	-2273	2260	4533	±2266
2,500	-2620	2375	4995	±2497
5,000	-2430	2675	5105	±2552
8,000	-2460	2730	5190	±2595
12,000	-2510	2750	5260	±2630
17,000	-2480	2850	5330	±2665
22,000	-2610	2770	5380	±2690
27,500	-2530	2920	5450	±2725
32,500	-2660	2960	5620	±2810
37,500	-2600	3045	5645	±2822
42,500	-2830	3255	6085	±3042

Cycles	$\Delta\epsilon$	Rg	ΔR
0	0	100.48	0.0
1	10		0.0021
5	48		0.0098
10	95		0.0195
30	200		0.0410
60	350		0.0728
100	545		0.1117
300	1670		0.3424

TEST # 5: (Continued)

Cycles	R_g	ΔR	
300	100.80	0.32	- Shifted to S/N
600	100.98	0.50	Resistance
1,000	101.15	0.67	meter
1,510	101.30	0.88	
2,500	101.88	1.40	
3,500	102.16	1.68	
5,000	102.67	2.19	
8,000	103.09	2.60	
12,000	103.88	3.40	
17,000	104.62	4.14	
22,000	105.25	4.77	
27,500	105.72	5.24	
32,500	106.25	5.77	
37,500	106.83	6.35	
42,500	107.60	7.12	
43,500	107.78	7.30	
43,900	107.93	7.45 *	

* Test terminated in order to preserve gage; fatigue crack in specimen had propagated almost to edge of gage.

TEST # 6: S/N Fatigue Data

Material: "Lucite 129" Acrylic Plastic

Design: Flat Bar

Serial No.: L-1

Strain Indicator: Strainsert HW-1

Gage Type: MA-01 Lot: A12AP15

Gage Factor Setting: 2.04

Clamping Block Position: # 1

Type Loading: Reverse Bending

Bending Rate: 500 CPM

Temperature: 71°F

Cycle No.	ϵ_c	ϵ_t	ϵ_T	ϵ_R
1	-.2273	3097	5370	±2685
5	-.2310	3080	5390	±2695

Cycle	Rg	ΔR	
0	100.25	0.00	
30	100.30	0.05	
61	100.33	0.08	
100	100.35	0.10	
300	100.58	0.33	
601	100.87	0.62	
1,000	101.05	0.80	
1,500	101.55	1.30	
2,500	101.88	1.63	
4,000	102.10	1.85	
6,000	103.08	2.83	
8,000	103.50	3.25	
10,000	103.77	3.52	
15,000	104.50	4.25	
20,000	105.00	4.75	
25,000	105.58	5.33	
30,000	106.05	5.80	
40,000	106.83	6.58	
49,528	107.90	7.65	Specimen failed at gage tip

TEST # 7: S/N Fatigue Data

Material: "Lucite 129" Acrylic Plastic

Design: Flat Bar

Serial No.: L-2

Strain Indicator: Strainsert HM-1

Gage Type: MA-01 Lot: Z-A12AP21

Gage Factor Setting: 2.04

Clamping Block Position: # 2

Bending Rate: Not Recorded, Random Rates (500-1080 CPM)

Temperature: 70°F

Cycle No.	ϵ_c	ϵ_t	ϵ_T	ϵ_s
1	-3455	3470	6925	±3463
5	-2955	3995	6950	±3475
1000	-3028	4105	7133	±3566

Cycle	Rg	ΔR	
0	100.32	0.00	
1	100.35	0.03	
5	100.40	0.08	
30	100.50	0.18	
60	100.60	0.28	
100	100.69	0.37	
300	101.12	0.80	
600	101.76	1.44	
1,000	102.15	1.83	
3,000	103.80	3.48	
6,000	105.12	4.80	
10,000	105.84	5.52	
10,690	105.90	5.58	Specimen failed at gage tip.

TEST # 8: S/N Fatigue Data

Material: "Lucite 129" Acrylic Plastic

Design: Flat Bar

Serial No.: L-3

Strain Indicator: Strainsert HW-1

Gage Type: NA-01 Lot: Z-A12AP21

Gage Factor Setting: 2.04

Clamping Block Position: # 3

Bending Rate: Not Recorded, Random Rates (500-1080 CPM)

Temperature: 70°F

Cycle No.	ϵ_c	ϵ_t	ϵ_T	ϵ_R
1	-4465	5560	10,025	±5012
5	-4460	5570	10,030	±5015

Cycle	Rg	ΔR	
0	100.00	0.00	
1	100.00	0.00	
5	100.23	0.23	
10	100.28	0.28	
30	100.48	0.48	
60	100.60	0.60	
100	100.92	0.92	
200	101.48	1.48	
400	102.04	2.04	
610	102.66	2.66	
1,002	103.88	3.38	
1,202	104.25	4.25	
1,700	105.05	5.05	
2,001	105.35	5.35	
3,001	106.12	6.12	
3,502	106.65	6.65	
4,012	106.79	6.79	
4,020	106.88	6.88	Specimen failed at gage tip.

TEST # 9: S/N Fatigue Data

Material: "Lucite 129" Acrylic Plastic

Design: Flat Bar

Serial No.: L-4

Strain Indicator: Strainsert HW-1

Gage Type: NA-01 Lot: Z-A12AP21

Gage Factor Setting: 2.04

Clamping Block Position: # 2

Bending Rate: Variable: $0 < N < 50,000$ 660 CPM
$50,000 < N < 68,700$ 870 CPM

Temperature: 70°F

Cycle No.	ϵ_c	ϵ_t	ϵ_T	ϵ_R
1	-2700	2970	5670	±2835
5	-2710	2970	5680	±2840

Cycle	Rg	ΔR
1	100.20	0.00
5	100.30	0.10
10	100.34	0.14
32	100.40	0.20
60	100.46	0.26
100	100.50	0.30
302	100.76	0.56
600	101.11	0.91
1,000	101.49	1.29
1,500	101.88	1.68
2,003	102.04	1.84
3,001	102.31	2.11
4,000	102.58	2.38
6,000	103.00	2.80
8,002	103.90	3.70
10,001	104.12	3.92
12,502	104.74	4.54

TEST # 9: (Continued)

Cycle	Rg	ΔR
15,000	104.95	4.75
20,000	105.27	5.07
30,000	105.70	5.50
40,016	105.97	5.77
50,000	106.18	5.98
60,000	107.66	7.46
68,700	107.86	7.66

Specimen failed at clamping block.

TEST # 10: S/N Fatigue Data

Material: "Lucite 129" Acrylic Plastic

Design: Flat Bar

Serial No.: L-5

Strain Indicator: Strainsert HW-1

Gage Type: NA-01 Lot: Z-A12AP21

Gage Factor Setting: 2.04

Clamping Block Position: # 0 (0.75" away from # 1)

Bending Rate:

$0 < N < 130,000$	500 CPM
$130,000 < N < 200,000$	660 CPM
$200,000 < N < 550,000$	1080 CPM

Cycle No.	ϵ_c	ϵ_t	ϵ_T	ϵ_R
1	-1570	2240	3810	±1905
5	-1610	2210	3820	±1910
10,000	-	-	3860	±1930
50,000	-	-	3930	±1965

Cycle	Rg	ΔR
0	100.35	0.00
1	100.35	0.00
5	100.37	0.02
100	100.45	0.10
500	100.53	0.18
1,003	100.60	0.25
3,000	100.87	0.52
6,000	101.18	0.83
10,000	101.70	1.35
20,008	102.25	1.95
30,000	102.50	2.15
40,000	102.75	2.40

TEST # 10: (Continued)

Cycle	Rg	ΔR	
50,000	103.05	2.70	
65,000	103.15	2.80	
100,000	103.79	3.44	
130,000	104.63	4.28	
170,100	105.34	4.99	
200,000	106.15	5.80	
250,000	106.47	6.12	} 30 minutes elapsed
250,000	107.36	7.01	
300,000	108.30	7.95	} 20 minutes elapsed
350,000	109.00	8.65	
350,000	109.47	9.12	
400,000	110.88	10.53	
450,000	112.19	11.84	} 20 hours elapsed
450,000	112.35	12.00	
500,000	115.06	14.71	
550,000	118.20	17.85	

Test terminated because of large value of ΔR.

TEST # 11: Effect of Time on S/N Fatigue Gage Resistance

Material: Aluminum 2024-T4

Design: Flat Bar

Strain Indicator: Strainsert HW-1

Gage Type: NA-01 Lot: A12AP13 or A12AP15

Type Loading: Reverse Bending

Strain Level: $\pm 1500 \mu\epsilon$

Gage # 1:

N	Rg	ΔR	Date
872,000	102.62	2.62*	April 1966
872,000	103.40	3.40	April 1967

Gage # 2:

N	Rg	ΔR	Date
872,000	102.62	2.62	April 1966
872,000	103.89	3.89	April 1967

* Triebes (31) assumed the initial resistance of his gages as 100 ohms since the manufacturer states that the gage resistance is 100.0 $\pm$ .2 ohms.

F. REFERENCES

1. Anderson, John R., "Copper-Nickel Alloys", Metallurgy Thesis M.S., MIT (1946).

2. Avery, Donald H., "Deformation and Fatigue in Copper Alloys", Metallurgy Thesis Sc-D, MIT (1962).

3. Bennett, J. A., "The Effect of a Fatigue Crack on the Fatigue Strength of an Aluminum Alloy", Naval Engineers Journal, Vol. 78, No. 1 (February 1966), p. 41-44.

4. Boeing Company, "Fatigue Life Gage Development Program", Report 78814-66-7, October 18, 1966.

5. Chalmers, Bruce and King, R., (eds.), "The Stored Energy of Cold Work", Progress in Metal Physics 7, Pergamon Press: New York (1958), p. 247-358.

6. Chalmers, Bruce and King, R., (eds.), "Work Hardening of Metals", Progress in Metal Physics 8, Pergamon Press: New York (1959), p. 1-105.

7. Chironis, N. P., "Changes in Strain Gages", Product Engineering, Vol. 36, No. 25, December 6, 1965, p. 33-38.

8. Clark, J. O. E., "The Etching of Printed Circuit Boards", Marconi Review, Third Quarter, Vol. 24, 1961, p. 134.

9. Cohen, J. B. and Bever, M. B., "Electrical Resistivity of Polycrystalline Cu_3Au", Transactions AIME, 218 (1960), p.155.

10. Dahl, O. Z., Metallkunde, Vol. 28 (1936), p. 133.

11. Ebner, M. L. and Backofen, W. A., "Fatigue in Single Crystals of Copper", Transactions AIME, 215 (1959), p. 510.

12. Fricke, W. G. Jr., "Fatigue Gages of Aluminum Foil", ASTM Materials Research and Standards, Vol. 2, No. 4, April 1962, p. 268-269.

13. Furuichi, H., Fuji, T., and Mizukawa, K., "Structural Change During the Fatigue of Close-Packed Hexagonal Metal", Proceedings of the Eight Japan Congress on Testing Materials, The Society of Materials Science, Japan, Kyoto, 1965.

14. Gibbons, W. G., "Strain-Cycle Fatigue of 70-30 Copper-Nickel", Journal of Basic Engineering, Transactions of the ASME, Vol. 88, No. 2, June 1966, p. 552-554.

15. Harting, Darrell R., "Fatigue Life Gaging Methods", U.S. Patent Office No. 3,272,003, September 13, 1966.

16. Herting, D. R., "The S/N Fatigue Life Gage: A Direct Means of Measuring Cumulative Fatigue Damage," Experimental Mechanics, Vol. 6, No. 2 (February 1966), p. 19A-24A.

17. Horne, Robert S., "A Feasibility Study for the Development of a Fatigue Damage Indicator", Technical Report AFFDL-TR-66-113, August 1966. (unofficial).

18. Hunter, M. S. and Fricke, W. G. Jr., "Effects of Alloy Content on the Metallographic Changes Accompanying Fatigue", Proceedings, American Society for Testing Materials, Vol. 55, 1955, p. 942.

19. Klemens, P. G., "The Failure of Matthiessen's Rule For Heavily Deformed Alloys", Australian Journal of Physics, 6 (1953), p. 122.

20. Manson, S. S., "Fatigue: A Complex Subject - Some Simple Approximations", Experimental Mechanics, Vol. 5, No. 7, p. 193-226 (July 1965).

21. Marin, Joseph, Pao, Yoh-Hon and Cuff, George, "Creep Properties of Lucite and Plexiglas for Tension, Compression, Bending and Torsion", Transactions of the ASME, July, 1951, p. 705-719.

22. Mott, N. F., "The Behavior of Metals Under Reversed Stresses", Dislocations and Mechanical Properties of Crystals, An International Conference held at Lake Placid, September 6-8, 1956, p. 458-478.

23. Oldroyd, P. W. J., Burnes, D. J. & Benham, P. P., Paper 2, Applied Mechanics Convention 1966, Cambridge, 4-6 April, Proceedings of Institution of Mechanical Engineers, 1966, Vol. 180, pt. 3 I.

24. "Precision Strain Gages", Catalog No. 20, W. T. Bean, Inc., Detroit, Mich.

25. Rohrbach, C. C. and Czaika, N., "Studies of the Fatigue Behavior of Strain Gages", Materialprüfung, (20 April, 1961).

26. S/N Fatigue Life Gage Applications Manual, Micro-Measurements, Inc., Romulus, Michigan, 1st Edition, (August, 1966).

27. Skagg, C. W., "Photo Etching Thin-Film Circuits", Electronics, Vol. 37, No. 18, 15 June 1964, p. 94-98.

28. Swann, P. R., "Stress-Corrosion Failure", Scientific American, No. 214, (February 1966), p. 72.

29. Society of Nondestructive Testing, Nondestructive Testing Handbook, Vol II. New York; Ronald Press Company, 1959, p. 54-22.

30. Thompson, N., "Some Observations on the Early Stages of Fatigue Fractures", Proceedings of an International Conference on the Atomic Mechanism of Fracture, Swampscott, Mass. April 12-16, 1959, p. 354-375.

31. Triebes, Carl J. Jr., "An Investigation of the S/N Fatigue Gage", Naval Architecture and Marine Engineering Thesis M. S., MIT (1966).

32. Wadsworth, N. J., "Energy Dissipation During Fatigue Tests", Dislocation and Mechanical Properties of Crystals, An International Conference held at Lake Placid, September 608, 1956, p. 479-491.

33. Webeler, Rayjor, "Formation of Cold-Worked Regions in Fatigue Metal", Journal of Metals, Transactions AIME, (February, 1955), p. 408-411.

34. Wood, W. A., "Experimental Approach to Basic Study of Fatigue", Columbia University Department of Civil Engineering and Engineering Mechanics Technical Report No. 24, August 1965.